 doi:10.20944/preprints202009.0532.v1

Human tendon repair following injection of autologous, unmodified stem cells: a comprehensive immunohistochemical evaluation

Eckhard U. Alt[1,2,3] | *Ralf Rothoerl*[1] | *Matthias Hoppert*[1] | *Hans-Georg Frank*[4] | *Christopher Alt*[5] | *Christoph Schmitz*[4]

[1] *Isar Klinikum, Munich, Germany*
[2] *Sanford Health, Sioux Falls, SD, USA*
[3] *InGeneron, Inc., Houston, TX, USA*
[4] *Chair of Neuroanatomy, Institute of Anatomy, Faculty of Medicine, LMU Munich, Munich, Germany*
[5] *InGeneron GmbH, Munich, Germany*

Key words: adipose derived regenerative cells; ADRCs; efficacy; point of care treatment; stem cells; stromal vascular fraction; tendon healing without scar formation; tendon regeneration

Current clinical treatment options for symptomatic rotator cuff tear offer only limited potential for true tissue healing and improvement of clinical results. In animal models, injections of adult stem cells isolated from adipose tissue into tendon injuries evidenced histological regeneration of tendon tissue. However, it is unclear whether such beneficial effects could also be observed in a human tendon treated with autologous, adipose derived regenerative cells. Here we demonstrate, for the first time, a comprehensive histological and immunohistochemical analysis of the biopsy of a supraspinatus tendon of a 66-year-old subject with traumatic rotator cuff injury, taken ten weeks after local injection of fresh, uncultured, autologous, adipose derived regenerative cells (UA-ADRCs), prepared at the point of care. Our analysis demonstrated clear evidence towards regenerative healing of the injured supraspinatus tendon. Of note, no formation of adipocytes was observed. These findings indicate that injected autologous, unmodified stem cells can indeed form new tendon tissue and regenerate an injured human tendon.

Correspondence
Dr. Eckhard U. Alt MD, PhD
IsarKlinikum Munich
Sonnenstr. 24
80331 Munich
Germany
Phone: +1-832-853-3898
e.alt@biomed-science.com

Preprints (www.preprints.org) | NOT PEER-REVIEWED | Posted: 23 September 2020 doi:10.20944/preprints202009.0532.v1

ABSTRACT

Current clinical treatment options for symptomatic rotator cuff tear offer only limited potential for true tissue healing and improvement of clinical results. In animal models, injections of adult stem cells isolated from adipose tissue into tendon injuries evidenced histological regeneration of tendon tissue. However, it is unclear whether such beneficial effects could also be observed in a human tendon treated with autologous, adipose derived regenerative cells. Here we demonstrate, for the first time, a comprehensive histological and immunohistochemical analysis of the biopsy of a supraspinatus tendon of a 66-year-old subject with traumatic rotator cuff injury, taken ten weeks after local injection of fresh, uncultured, autologous, adipose derived regenerative cells (UA-ADRCs), prepared at the point of care. Our analysis demonstrated clear evidence towards regenerative healing of the injured supraspinatus tendon. Of note, no formation of adipocytes was observed. These findings indicate that injected autologous, unmodified stem cells can indeed form new tendon tissue and regenerate an injured human tendon.

Preprints (www.preprints.org) | NOT PEER-REVIEWED | Posted: 23 September 2020 doi:10.20944/preprints202009.0532.v1

INTRODUCTION

Fresh, uncultured, autologous, adipose derived regenerative cells (UA-ADRCs) are prepared at the point of care (in some publications these cells are also called stromal vascular fraction; SVF) (Winnier et al., 2019; Alt et al., 2020). Unlike some other cell preparations currently under investigation for use in regenerative medicine (including bone marrow derived cells, allogenic stem cells, amniotic cells or induced pluripotent stem cells) UA-ADRCs are derived from the same subject, not expanded in culture and are less exposed to factors that could affect their safety and efficacy (Cossu et al., 2018; Alt et al., 2020). Furthermore, UA-ADRCs do not share the risk of potentially developing tumors and immunological defensive reactions (Winnier et al., 2019; Alt et al., 2020). While less than 0.1% of the total population of bone marrow nucleated cells represent true stem cells, UA-ADRCs contain up to 10% multipotent cells out of the total population of injected cells (Alt et al., 2020). Additionally, harvesting adipose tissue is considered less invasive than harvesting bone marrow (Bayek et al., 2015).

Symptomatic, partial-thickness rotator cuff tear (sPTRCT) is one of the most prevalent shoulder disorders in adults, often leading to persistent pain, loss of function and occupational disability (Matthewson et al., 2015). Current non-surgical and surgical treatment options to address sPTRCT do not necessarily have the potential to replace damaged tendon tissue, and often do not improve clinical results (Coombes et al., 2010). Treatment with corticosteroid injection can provide short-term pain relief but may not modify the course of the disease (Coombes et al., 2010; Ramirez et al., 2014). Two recent studies (a systematic review (Hurley et al., 2019) and a randomized controlled trial (RCT) (Schwitzguebel et al., 2019)) found that injections of platelet rich plasma might be of limited benefit in non-operative treatment of rotator cuff disease. Other authors demonstrated that results from surgical interventions may not exceed those obtained with conservative management (Kukkonen et al., 2014).

A recent in vitro study demonstrated that fresh UA-ADRCs may be superior to cultured adipose derived stem cells (ASCs) as trophic mediators for tendon healing (Polly et al., 2019). In addition, we recently published the first-in-human pilot RCT on treating sPTRCT with UA-ADRCs (Hurd et al., 2020). In the latter study subjects treated with UA-ADRCs showed significant clinical improvement compared to subjects treated with corticosteroid injection ($p < 0.05$) at six and twelve months post treatment (Hurd et al., 2020).

The aim of the present, comprehensive immunohistochemical analysis of a biopsy of the supraspinatus tendon of a subject suffering from sPTRCT that was taken ten weeks after injection of UA-ADRCs is to provide novel insights into mechanisms of tendon regeneration following stem cell injection in humans. To our knowledge, this is the first investigation of a biopsy taken from a human tendon after application of unmodified, autologous stem cells.

MATERIALS AND METHODS

Subject and Ethics statement

This study is a single self-experiment with the subject's consent. The subject was the first author of this study, Dr. Eckhard U. Alt, MD, PhD. Single self-experiments with the subject's unrestricted and free will formation are exempt from approval of an Institutional Review Board in Germany (c.f. Hanleyet al., 2019). It was Dr. Alt himself who initiated his own treatment, taking the biopsy and all investigations. Dr. Alt gave informed consent to participate in this study.

The then 66-year-old subject had a bicycle accident in October 2016, during which his right shoulder hit the street first. He experienced intense pain in his right shoulder with pain radiating to his back, upper arm and elbow. Magnetic resonance imaging (MRI) of his right shoulder evidenced a combined partial-thickness tear of the supraspinatus tendon (PASTA), an intramuscular cyst of the supraspinatus muscle and an initial partial-thickness tear of the infraspinatus tendon (Fig. 1a-d).

On day 18 following his injury (day 16 after MRI diagnosis) the subject was treated by transcutaneous injection of UA-ADRCs into the supraspinatus tendon lesion under fluoroscopic control. As part of this process, approximately 100 g of abdominal adipose tissue was harvested by liposuction, from which approximately 75×10^6 UA-ADRCs were isolated within less than two hours using the Transpose RT system (InGeneron, Houston, TX, USA). Detailed characterizations of cells isolated from human adipose tissue using the Transpose RT system are available in the literature (Winnier et al., 2019; Alt et al., 2020; Hurd et al., 2020). The UA-ADRCs were injected into the injured supraspinatus tendon immediately after isolation. The infraspinatus tendon was not treated at this time.

A control MRI performed ten weeks post injection of the subject's own stem cells showed substantial reduction of trauma-related bruising and the formation of a hyperintense structure at the *supra*spinatus site of injection of the cells (Fig. 1e-h). Using a rabbit Achilles tendon defect model we recently demonstrated that development of hyperintense structures found in MRI scans at the position of the injection of UA-ADRCs represent newly formed, well organized, firm connective tissue with high cell density (Alt et al., 2020).

On the other hand, the patients control MRI indicated aggravation of his *infra*spinatus tendon tear of the right shoulder that required surgical revision. During this operation a biopsy from the supraspinatus tendon (at the position of the hyperintense structure that was seen on the MRI scans) was taken, which was then prepared for histological and immunohistochemical analysis.

Preprints (www.preprints.org) | NOT PEER-REVIEWED | Posted: 23 September 2020 doi:10.20944/preprints202009.0532.v1

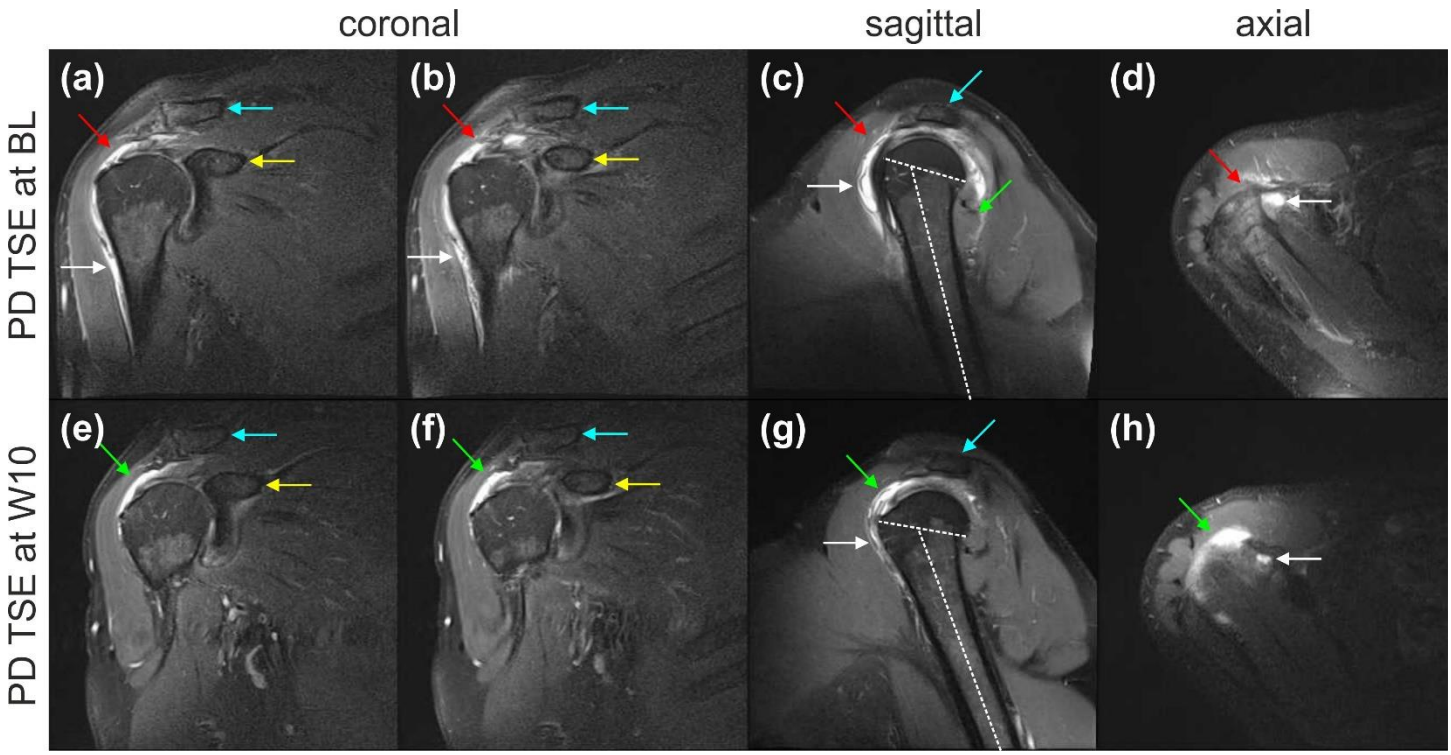

Figure 1. Magnetic resonance imaging (MRI) scans of the right shoulder of the investigated subject. The panels show coronal (a, b, e, f), sagittal (c, g) and axial (d, h) proton density weighted, fat saturated Turbo Spin Echo (PD FS TSE) 1.5 T MRI scans at baseline (BL) (a-d) and ten weeks post injection of UA-ADRCs (W10) (e-h) (matrix 320×320; slice thickness 3 mm; inter-slice gap 0.3 mm; echo time [TE] 37 ms; repetition time [TR] 2450 ms at BL and 3480 ms at W10 post injection). The white arrows in (a-d, g, h) indicate trauma-related bruising that disappeared fully (e, f) or partially (g, h) between BL and W10 post injection. The green arrows in (e-h) point to a hyperintense structure at the position of the supraspinatus tendon that was found at W10 post injection but not at BL (red arrows in (a-d)). The blue arrows in (a, b, e, f) indicate the clavicula, the yellow arrows in (a, b, e, f) the coracoid process of the scapula, and the blue arrows in (c, g) the acromion. The angle between the dotted lines is the same in (c, g).

Histology and immunohistochemistry

After fixation in 4% formaldehyde the two parts of the biopsy were separately embedded in paraffin and cut into 4 µm-thick tissue sections that were mounted on glass slides and stained with Azan trichrome stain or processed with immunohistochemistry. The latter was performed on de-paraffinized and rehydrated sections that were washed with phosphate buffered saline (PBS) containing Tween 20 (Sigma Aldrich, St. Louis, MO, USA). After antigen retrieval and / or enzymatic and / or chemical pretreatment the slides were blocked with different solutions for 15 to 60 minutes at room temperature (details are provided in Table 1). Then, sections were incubated with primary antibodies for the detection of aggrecan, CD34, CD68, Ki-67, laminin, MMP-2, MMP-9, procollagen 1, tenomodulin, type I collagen and type II collagen as summarized in Table 1.

Antibody binding was detected with the Vectastain Elite ABC Kit Peroxidase (HRP) (Vector Laboratories, Burlingame, CA, USA) with a secondary antibody incubation of 30 minutes for all slides (Table 1). Visualization of peroxidase activity was performed using diaminobenzidine (Vector Impact DAB chromogen solution; Vector Laboratories), resulting in a brown staining product. Mayer's hematoxylin was used for counterstaining the sections. In order to perform specificity controls primary antibodies were omitted and replaced with PBS. Microscopic evaluations were performed by E.U.A., C.A. and C.S.

Photography

All photomicrographs were produced by digital photography. Except for Figure 3 this was done using an automated scanning microscopy workstation, consisting of a M2 AxioImager microscope (Zeiss, Goettingen, Germany), 40x Plan-Apochromate objective (numerical aperture [N.A.] = 0.95; Zeiss), two-axis computer controlled stepping motor system (4″ × 3″ XY; Prior Scientific, Jena, Germany), focus encoder (Heidenhain, Traunreut, Germany) and color digital camera (AxioCam MRc; 2/3" CCD sensor, 1388 × 1040 pixels; Zeiss). The whole system was controlled by the software Stereo Investigator (Version 11.06.2; MBF Bioscience, Williston, VT, USA). On average approximately 800 three-dimensional (3D) images with averaged 25 image planes and distance of 1 µm between the image planes) were captured for the composite in each Figure 2a,c,h,j and Figures 4a – 13a. These images were made into one montage each using the Virtual Slide module of the StereoInvestigator software; the size of the resulting 3D virtual slides varied between 1.7 and 6.7 GB. The high-power photomicrographs shown in Figure 2d-g,i,k and Figures 4b-g – 13b-g were

created from the virtual slides using the software Biolucida Viewer (Version 2019.3.4; MBF Bioscience).

Figure 3 was produced using a Zeiss Axiophot Microscope equipped with an Axiocam HRc digital camera (2/3" CCD sensor, 1388 × 1040 pixels; Zeiss) that was controlled by the software Zeiss Axiovision SE64 (Rel. 4.9.1 SP2). The images were taken in transmitted light mode without (Fig. 3a) or with polarized light (Fig. 3b) using a Zeiss Plan-Neofluar 5x objective (N.A. = 0.15). The polarized image was taken in black and white mode of the digital camera. Illumination was adjusted using the automatic measurement function of the Zeiss Axiovision software.
The final figures were constructed using Corel Photo-Paint X7 and Corel Draw X7 (both versions 20.1.0.708; Corel, Ottawa, Canada). Only adjustments of contrast and brightness were made using Corel Photo-Paint, without altering the appearance of the original materials.

Table 1. Characteristics of the primary antibodies used in this study.

Antibody (anti…)	Characteristics
aggrecan	IgG1, mouse, monoclonal / 12/21/1-C-6 / DSHB[a] / Protease XIV and Chondroitinase AC / Bloxall SP-6000[b], NHS S-2000[b], 1:20 / 1:5, RT, 4h / HaM IgG BA-2000[b], 1:200
CD34	IgG1, mouse, monoclonal / QBEnd-10 / Thermo Scientific (Waltham, MA, USA) / - / 3% H_2O_2 in Methanol, NGS S-1000[b] 5 % / 1:900, 4° C, ON / GaM IgG BA-9200[b], 1:200, in 2% BSA/PBS
CD68	KP1- IgG1 kappa, mouse, monoclonal / M0814 / Dako (Glostrup, Denmark) / boiling in citrate buffer (pH 6) / Bloxall SP-6000[b], NHS S-2000[b], 1:20 / 1:100, 4° C, ON / HaM IgG BA-2000[b], 1:200
Ki-67	MIB-1 IgG1 kappa, mouse, monoclonal / M7240 / Dako / boiling in citrate buffer (pH 6) / Bloxall SP-6000[b], NHS S-2000[b], 1:20 / 1:75, 4° C, ON / HaM IgG BA-2000[b], 1:200
laminin	IgG2a, mouse, monoclonal / 2E8 / DSHB[a] / - / 1:5/1:10, RT, 30 min / HaM IgG BA-2000[b], 1:200
MMP-2	IgG, rabbit, polyclonal / 97779 / Abcam (Cambridge, UM) / - / Bloxall SP-6000[b], NHS S-2000[b], 1:20 / 1:100, 4° C, ON / GaR IgG BA-1000[b], 1:200
MMP-9	IgG, rabbit, polyclonal / 38898 / Abcam / - / Bloxall SP-6000[b], NHS S-2000[b], 1:20 / 1:100, 4° C, ON / GaR IgG BA-1000[b], 1:200
procollagen 1	IgG1 mouse, monoclonal / SP1.D8 / DSHB[a] / Boiling in citrate buffer (pH 6) / Bloxall SP-6000[b], NHS S-2012[b], 2.5% / 1:10, 4° C, ON / HaM IgG BA-2000[b], 1:200
tenomodulin	IgG rabbit, polyclonal / 203676 / Abcam / - / 3%H_2O_2 in Methanol, NHS S-2012[b], 2.5% / 1:200/ 1:500, RT, 30 min / HaR IgG BA-1100[b], 1:200
Type I collagen	IgG1 mouse, monoclonal / C2456 / Sigma-Aldrich (St. Louis, MO, USA) / Protease XIV and Hyaluronidase / Bloxall SP-6000[b], NHS S-2000[b], 1:20 / 1:2000, RT, 30 min / HaM IgG BA-2000[b], 1:200
Type II collagen	MIgG2A kappa light chain, mouse, monoclonal / CIIC1 / DSHB[a] / Protease XIV and Hyaluronidase / Bloxall SP-6000[b], NHS S-2000[b], 1:20 / 1:6, RT, 30 min / HaM IgG BA-2000[b], 1:200

The table shows for each primary antibody the following: immunoglobuline isotype and clone status / name / manufacturer / demasking of antigens / blocking / dilution and incubation parameters / secondary antibody used to detect binding of the primary antibody). Notes: a, the antibodies 12/21/1-C-6 (developed by Dr. B. Caterson), 2E8 (developed by Dr. E.S. Engvall), SP1.D8 (developed by Dr. H Furthmayr) and CIIC1 (developed by Drs R. Holmdahl and K. Rubin) were obtained from the Developmental Studies Hybridoma Bank, created by the NICHD of the NIH and maintained at The University of Iowa, Department of Biology, Iowa City, IA, USA. b, provider: Vector Laboratories (Burlingame, CA, USA). Abbreviations: GaM, goat anti-mouse; GaR, goat anti-rabbit; HaM, horse anti-mouse; HaR, horse anti-rabbit; NHS, normal horse serum; NGS, normal goat serum; RT, room temperature; ON, overnight.

RESULTS

Analysis of the first part of the biopsy

Sections from the first part of the biopsy showed the following (due to the complexity of the results of the various investigations their specific interpretation is provided next to each finding, together with references to the relevant literature):

Azan trichrome staining demonstrated that this part of the biopsy mostly consisted of a region with elongated fibroblast-like cells (tenocytes) arranged in long and parallel chains between collagen fibers (Fig. 2a,b). Type 1 collagen is the most abundant collagen of the human body, present in tendons, ligaments, organ capsules and scar tissue, etc. (Mescher, 2018). Immunohistochemical detection of type I collagen (Fig. 2c-g; Fig. 3a) revealed five different regions within this part of the biopsy, characterized by (1) organized, slightly undulating type I collagen and high cell density (Fig. 2d; "1" in Fig. 3a) (this region represented most of the area of the section), (2) organized type I collagen with discernible crimp arrangement and a few cells (Fig. 2e; "2" in Fig. 3a), (3) organized type I collagen with discernible crimp arrangement and almost complete absence of cells (Fig. 2f; "3" in Fig. 3a), (4) almost complete absence of immunolabeling for type I collagen and a few, rounded cells (Fig. 2g; "4" in Fig. 3a) and (5) almost complete absence of immunolabeling for type I collagen but a high cell density ("5" in Fig. 3a).

Additional immunohistochemical analysis showed immunolabeling for aggrecan (Fig. 2h,i) but not for type II collagen (Fig. 2j,k). Aggrecan and type II collagen are markers of tissues with a fibrocartilaginous phenotype and thus, intermittent compressive load acting on the tendinous tissue (Benjamin and Ralphs, 1998). Specifically, the presence of aggrecan in a tendon increases its capacity to imbibe water and, thus, to withstand compression; type II collagen is the

typical collagen found in hyaline and various fibrous cartilages (Benjamin and Ralphs, 1998).

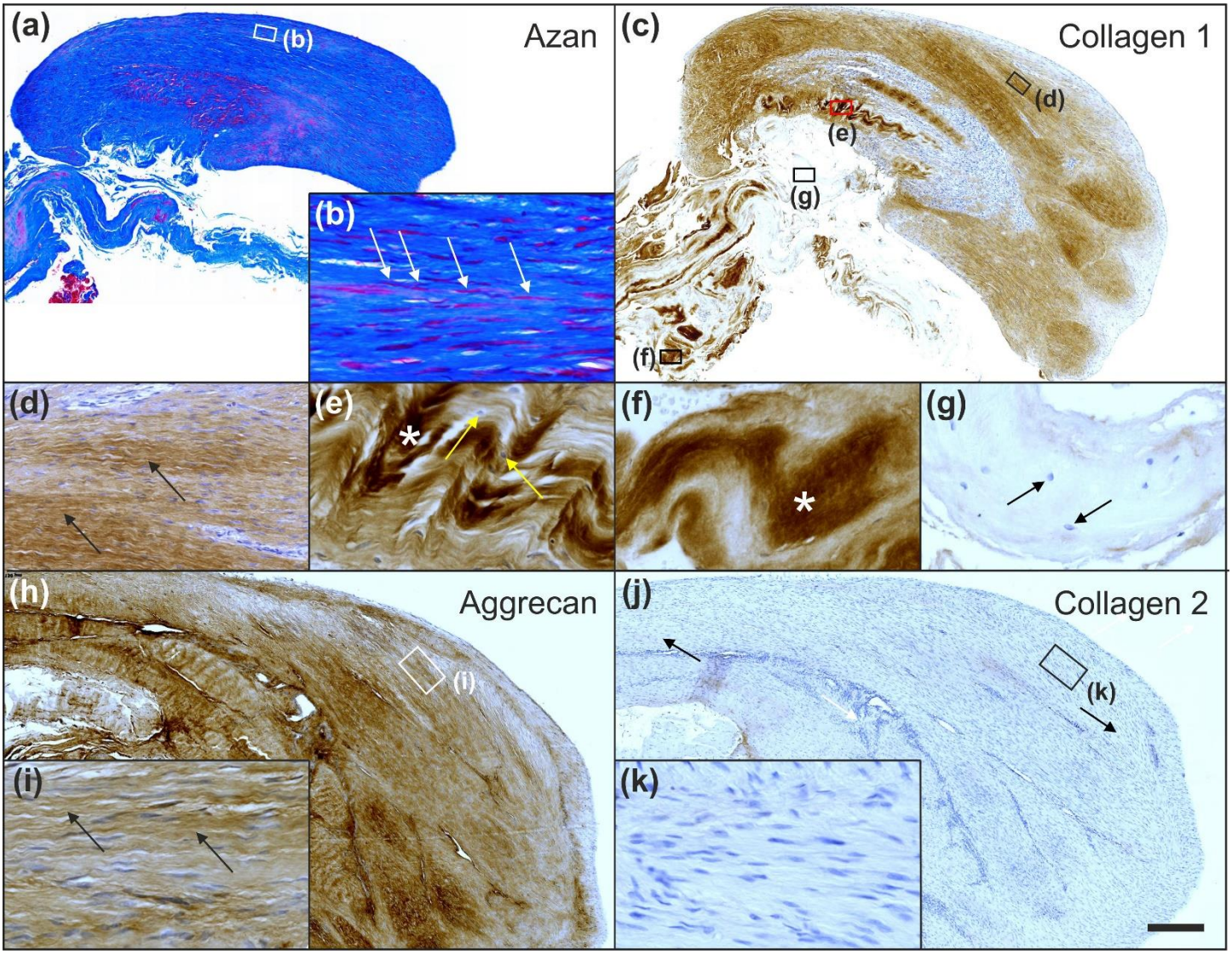

Figure 2. Histological and immunohistochemical analysis of representative sections from the first part of the biopsy that was investigated in this study. (a, b) Section stained with Azan trichrome stain; cells are in red and collagen is in blue. The inset in (a) indicates the position of the high-power photomicrograph displayed in (b). Note the elongated fibroblast-like cells (tenocytes) arranged in long and parallel chains between collagen fibers (white arrows in B). (c-g) Immunohistochemical detection of type I collagen in a section adjacent to the one shown in (a); counterstaining was performed with Mayer's hematoxylin. The insets in (c) indicate the position of the high-power photomicrographs displayed in (d-g), showing the following four different regions: (d) immunolabeling for organized, slightly undulating type I collagen (black arrows in d) and high cell density; (e) immunolabeling for organized type I collagen with discernible crimp arrangement (white asterisk in e) and a few cells (yellow arrows in e); (f) immunolabeling for organized type I collagen with discernible crimp arrangement (white asterisk in f) and absence of cells; and (g) absence of immunolabeling for type I collagen and a few, rounded cells (black arrows in g). The black asterisk in (b) indicates a region with almost complete absence of immunolabeling for type I collagen but a high cell density. (h-k) Immunohistochemical detection of aggrecan (h, i) and type II collagen (j, k) in other sections adjacent to the one shown in (a) of the same biopsy; counterstaining was also performed with Mayer's hematoxylin. The insets in (h) and (j) indicate the position of the high-power photomicrographs displayed in (i) and (k). The scale bar in (j) represents 250 µm in (a, c, h, j) and 50 µm in (b, d-g, i, k).

Collectively, the presence of immunolabeling for type I collagen and aggrecan and the absence of immunolabeling for type II collagen in the region of regenerative tendon tissue indicate that the latter was exposed to intermittent tensile load and probably slight intermittend compressive load, which is characteristic for the supraspinatus tendon (tensile load during contraction of the supraspinatus muscle; slight compressive load during adduction of the arm and wrapping the supraspinatus tendon around the humeral head).

Investigation of the section shown in Fig. 3a with polarization microscopy demonstrated a clear difference in collagen fiber birefringence between Regions 1 and 2, as well as absence of collagen fiber birefringence in Regions 4 and 5 (Fig. 3b).

Preprints (www.preprints.org) | NOT PEER-REVIEWED | Posted: 23 September 2020 doi:10.20944/preprints202009.0532.v1

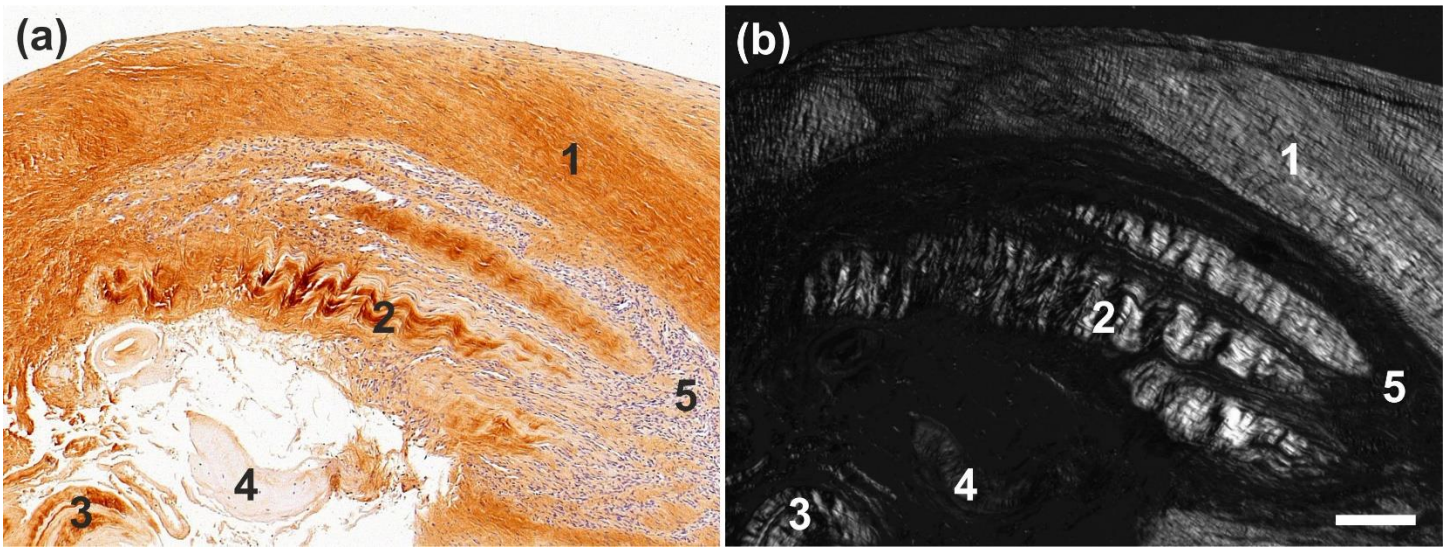

Figure 3. Histological and immunohistochemical analysis of representative sections from the first part of the biopsy that was investigated in this study. (a) Immunohistochemical detection of type I collagen in a representative section of the first part of the biopsy that was investigated in this study, showing the following five different regions (high-power photomicrographs are provided in Fig. 2): 1, organized, slightly undulating type I collagen and high cell density; 2, organized type I collagen with discernible crimp arrangement and a few cells; 3, organized type I collagen with discernible crimp arrangement and almost complete absence of cells; 4, almost complete absence of immunolabeling for type I collagen and a few, rounded cells; and 5, almost complete absence of immunolabeling for type I collagen but a high cell density. (b) Corresponding polarized light microscopic image of the same field of view. Note the clear difference in collagen fiber birefringence between Regions 1 and 2, and the absence of collagen fiber birefringence in Regions 4 and 5. The scale bar represents 200 µm in (a, b).

Analysis of the second part of the biopsy

A section from the second part of the biopsy that was stained with Azan trichome stain also showed regions with elongated fibroblast-like cells arranged in long and parallel chains between collagen fibers (Fig. 4a,e-g). In addition, regions with unorganized collagen with (Fig. 4b) or without (Fig. 4c) formation of microvessels were found, as well as a spot with very high density of cells and microvessels (Fig. 4d). Of note, no formation of any adipocytes was observed, indicating that the differentiation of stem cells (initially derived from adipose tissue) was guided by the new location and microenvironment. In the absence of adipose tissue the cells did not form adipose tissue but apparently followed the signaling coming from the injured tendon.

Based on the findings shown in Figure 4, sections from the second part of the biopsy were exposed to antibodies for the detection of CD34 (Fig. 5), Ki-67 (Fig. 6), tenomodulin (Fig. 7), type I procollagen (Fig. 8), type I collagen (Fig. 9), laminin (Fig. 10), matrix metalloproteinase 2 (MMP-2) (Fig. 11), MMP-9 (Fig. 12) and CD68 (Fig. 13), revealing for each of the regions shown in Figure 4a-g a different, complex pattern of immunolabeling (summarized in Table 2). Weakest immunolabeling was found in the regions with unorganized collagen (Fig. 4b,c), whereas strongest immunolabeling was observed in the spot with very high density of cells and microvessels (Fig. 4d).

CD34 is considered a common progenitor cell marker and is expressed by a wide range of cell types, including bone marrow hematopoietic stem cells, mesenchymal stem cells (MSCs) and endothelial progenitor cells (Marvasti et al., 2019). More than 50% of freshly isolated MSCs express the CD34 cell marker; however, human cultured MSCs are commonly immunonegative for CD34 (Dominici et al., 2006). Accordingly, the presence of CD34+ immunolabeling in endothelial cells of microvessels in Regions D and F of the second part of the investigated biopsy (Fig. 5d,f) indicate ongoing angiogenesis in highly specific regions of the investigated biopsy ten weeks post injection of UA-ADRCs. On the other hand, anti CD34 immunohistochemistry could not be used to assess the potential presence of injected UA-ADRCs and their non-endothelial descendants in the investigated biopsy.

Ki-67 is a cellular marker for proliferation (Scholzen and Gerdes, 2000). The presence of immunolabeling for Ki-67 in cells inside microvessel walls in Region D of the second part of the investigated biopsy (Fig. 6d) is in line with the presence of immunolabeling for CD34 in endothelial cells of microvessels in this region (Fig. 5d). Furthermore, it appears reasonable to hypothesize that immunolabeling for Ki-67 in cells outside microvessel walls in Region D (Fig. 6d) could indicate the presence of injected UA-ADRCs and their non-endothelial descendants in this region ten weeks post injection of UA-ADRCs; and immunolabeling for Ki-67 in cells with the characteristic morphology of tenocytes in Region F indicates tendon regeneration (Fig. 6f).

Preprints (www.preprints.org) | NOT PEER-REVIEWED | Posted: 23 September 2020 doi:10.20944/preprints202009.0532.v1

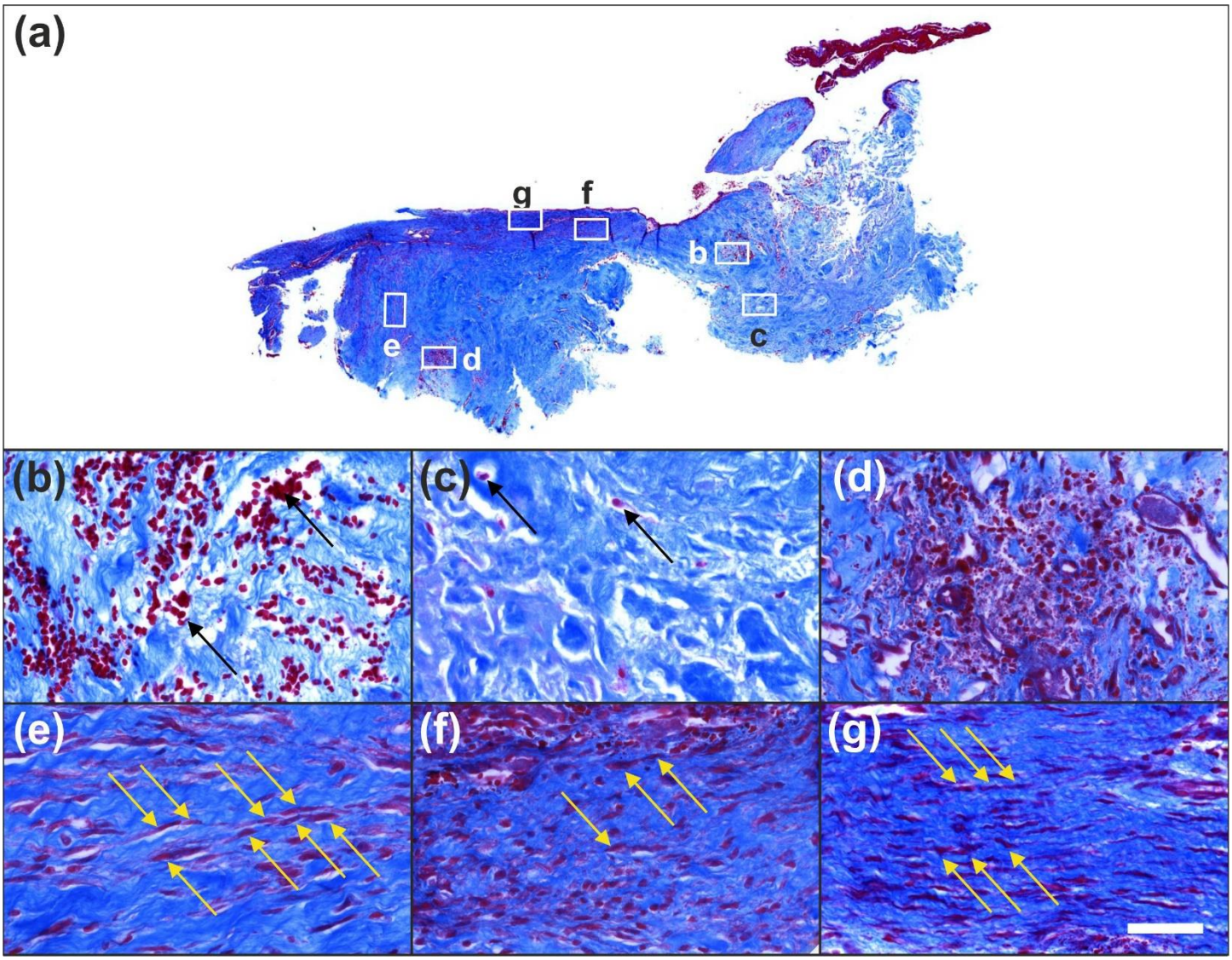

Figure 4. Histological analysis of a representative section of the second part of the biopsy that was investigated in this study. The section was stained with Azan trichrome stain; cells are in red and collagen is in blue. The insets in (a) indicate the position of the high-power photomicrographs displayed in (b-g), showing the following six different regions: (b) degenerative tendon tissue with formation of microvessels (the black arrows in (b) point to blood cells); (c) degenerative tendon tissue without formation of microvessels (the black arrows in (c) indicate rounded cells); (d) spot with very high density of cells and microvessels; (e) tendon tissue in the depth of the biopsy; (f) tendon tissue below an outer surface of the biopsy; and (g) tendon tissue at an outer surface of the biopsy (the yellow arrows in (e-g) point to elongated, fibroblast-like cells (tenocytes) arranged in long and parallel chains between collagen fibers). The scale bar in (g) represents 630 µm in (a) and 50 µm in (b-g).

Tenomodulin is a tendon-specific marker important for tendon maturation, with key implications for residing tendon stem/progenitor cells and the regulation of endothelial cell migration (Shukunami et al., 2001; Brandau et al., 2001; Dex et al., 2016). The abundant intracellular and extracellular presence of tenomodulin in Region D of the second part of the biopsy (Fig. 7d) is in line with the hypothesis that tendon regeneration observed in the investigated biopsy was 'orchestrated' from this region, further supporting the hypothesis that Region D in the second part of the investigated biopsy hosted injected UA-ADRCs and their descendants (c.f. Fig. 4d). On the other hand, the presence of tenomoduline immunopositive cells inside microvessels in Region B of the second part of the biopsy (Fig. 7b) may indicate an unsuccessful attempt of the body to endogenously initiate tendon regeneration by transferring corresponding cells via the blood stream into the injured/degenerative tissue.

Type I procollagen is a triple-stranded, rope-like molecule that is processed by enzymes outside the cell, followed by self-arrangement of the processed molecules into long, thin collagen fibrils that cross-link to one another in the extracellular space (Prockop et al., 1979a, 1979b). Accordingly, immunolabeling for type I procollagen in cells outside microvessel walls in Region D as well as in Regions E and F of the second part of the investigated biopsy (Fig. 8d-f) indicate that these regions were involved in tendon

Preprints (www.preprints.org) | NOT PEER-REVIEWED | Posted: 23 September 2020 doi:10.20944/preprints202009.0532.v1

regeneration in the investigated biopsy.

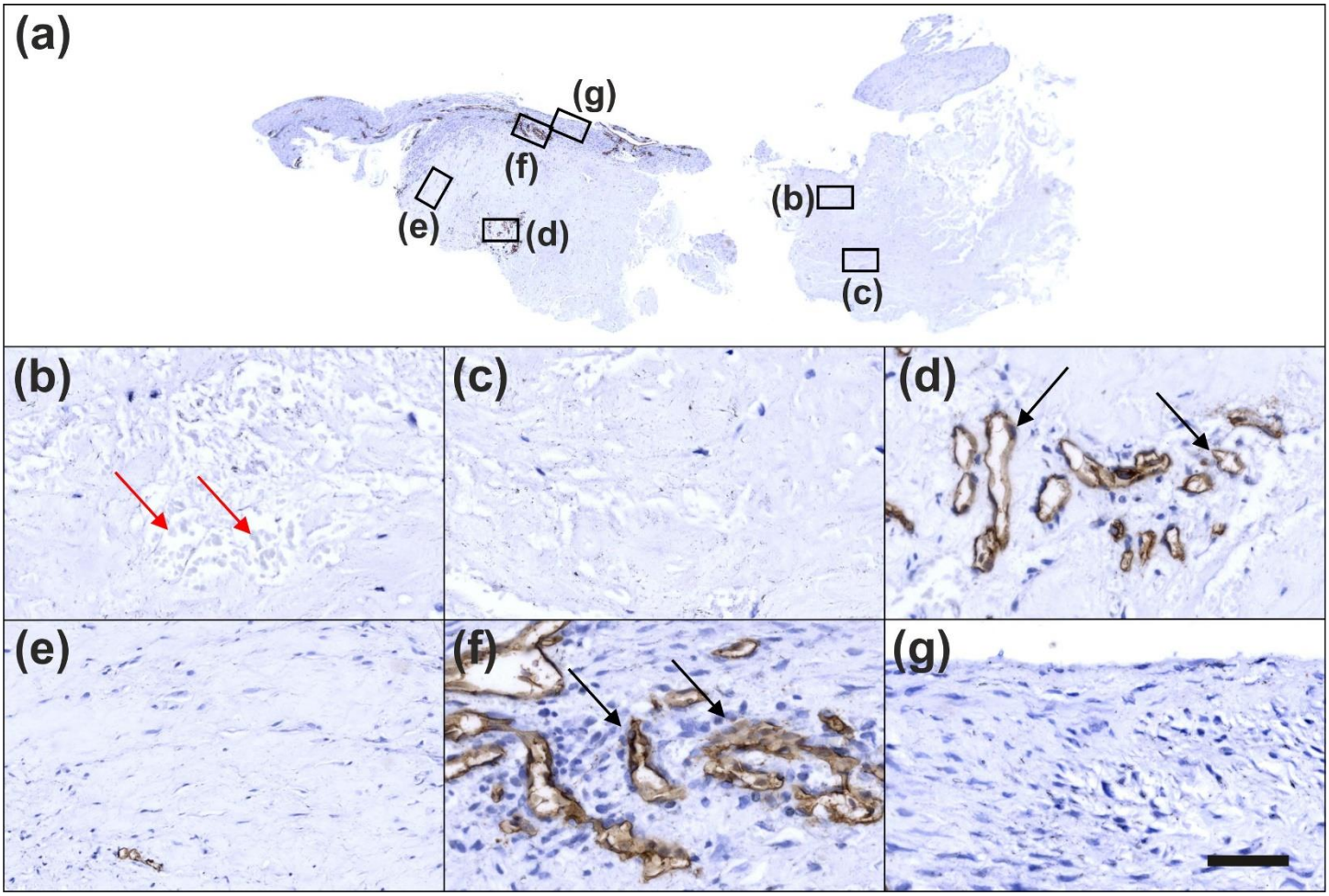

Figure 5. Immunohistochemical detection of CD34 in a section of the second part of the biopsy that was investigated in this study. The section was adjacent to the one shown in Figure 4(a); counterstaining was performed with Mayer's hematoxylin. The insets in (a) indicate the position of the high-power photomicrographs shown in (b-g), representing the same regions as the high-power photomicrographs shown in Figure 4(b-g). Immunolabeling for CD34 was found in endothelial cells of microvessels in Regions d and f (black arrows in (d, f)) but not in Regions b, c, e and g (the red arrows in (b) indicate cells inside a microvessel). The scale bar in (g) represents 630 µm in (a) and 50 µm in (b-g).

The finding of unorganized Type I collagen found in Regions D and E as well as of slightly undulating Type I collagen in Regions F and G of the second part of the investigated biopsy (Fig. 9d-e) indicates that these regions as well were involved in tendon regeneration, with Region G representing fully regenerated tendon tissue.

Laminin is an essential component of the extracellular matrix in soft tissues and modulates a number of cellular functions, including adhesion, differentiation and migration (Halper and Kjaer, 2014). An in vitro study on mouse embryonic stem cell migration found that laminin decreased cell aggregation and increased migration (Suh and Han, 2010). Another in vitro study on tenocytes isolated from injured rotator cuff tendons of human subjects concluded that an early increase in the expression of laminin could be beneficial to tendon healing by expediting cellular migration, attachement and growth (Molloy et al., 2006). Thus, the presence of intracellular and extracellular immunolabeling for laminin in Regions D and E of the second part of the investigated biopsy (Fig. 10d,e) are in line with the hypothesis that precursors of endothelial cells and tenocytes migrated from Region D (where they were generated) via Region E to Region F where tendon regeneration took place.

The interstitial collagenase MMP-2 catalyzes cleavage of collagen fibrils and soluble native type I collagen (Aimes and Quigley, 1995). A number of recent studies demonstrated that MMP-2 plays an important role in proliferation, migration and angiogenesis of MSCs (Almalki and Agrawal, 2016). Thus, the presence of intracellular and extracellular immunolabeling for MMP-2 in Regions D-F of the second part of the investigated biopsy (Fig. 11d-f) is in line with the hypothesis that precursors of endothelial cells and tenocytes migrated from Region D (where they were generated) via Region E to Region F where tendon regeneration took place. Of note,

MMP-2 was also positively associated with adipogenic and chondrogenic differentiation of MSCs (Rezzaet al., 2014), which was not observed in this study. This was most probably due to the fact that the corresponding studies were performed in vitro with single (or only a few) stimulating and inhibiting markers, whereas in vivo under the conditions of tissue injury the fate of MSCs depends on constant induction of differentiation and re-confirmation by complex signals released and communicated from the local microenvironment (Dong et al., 2015; Wabik and Jones, 2015; Alt et al., 2020).

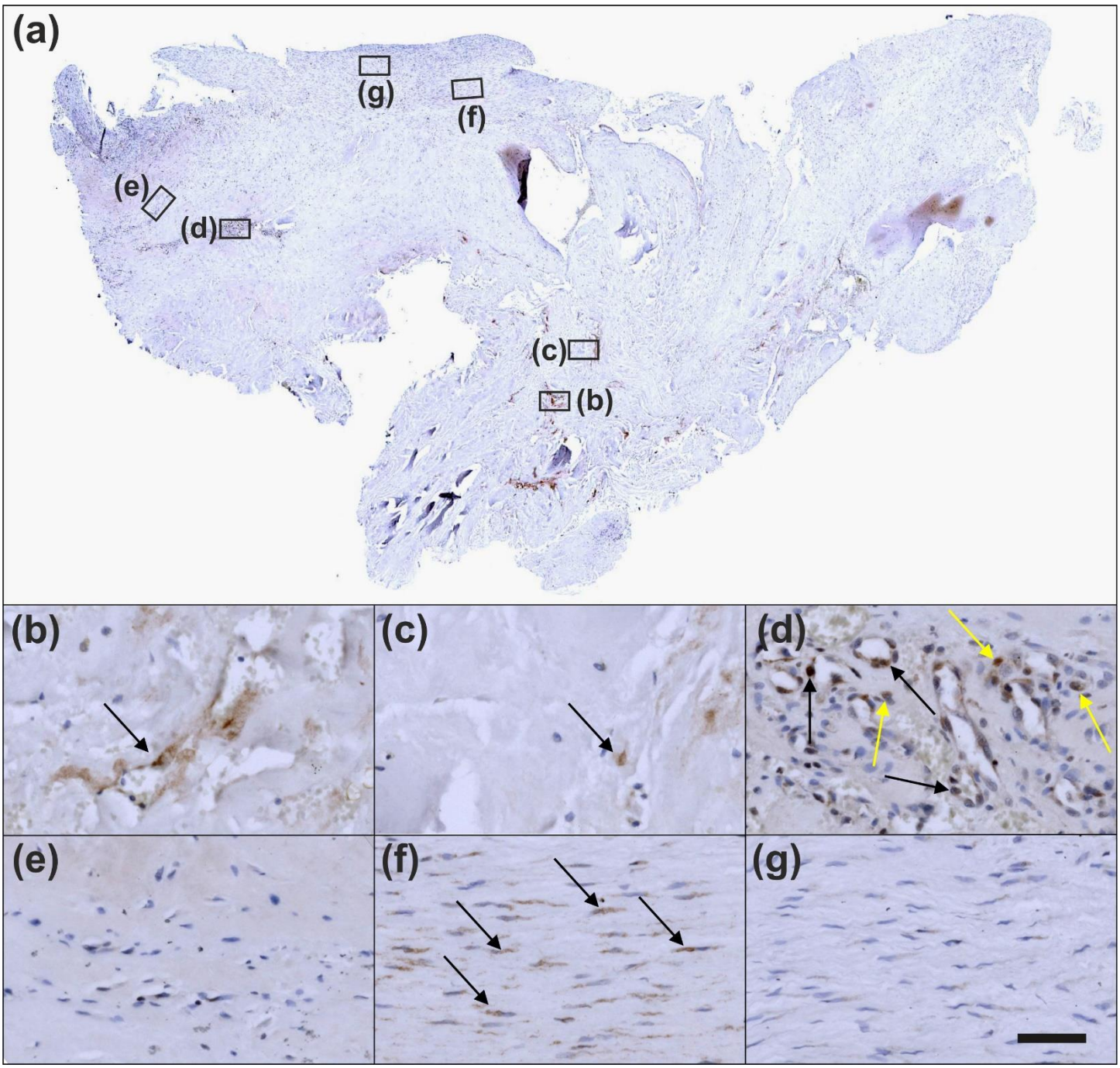

Figure 6. Immunohistochemical detection of Ki-67 in a section of the second part of the biopsy that was investigated in this study. The section was adjacent to the one shown in Figure 4(a); counterstaining was performed with Mayer's hematoxylin. The insets in (a) indicate the position of the high-power photomicrographs shown in (b-g), representing the same regions as the high-power photomicrographs shown in Figure 4(b-g). Immunolabeling for Ki-67 was found in very few cells in Regions b and c (black arrows in (b, c)), in many cells inside and outside microvessel walls in Region d (black and yellow arrows in (d)), and in particular in elongated cells in a chain-like arrangement in Region f (black arrows in (f)). No Ki-67 immunolabeling was found in Regions e and g. The scale bar in (g) represents 630 µm in (a) and 50 µm in (b-g).

Preprints (www.preprints.org) | NOT PEER-REVIEWED | Posted: 23 September 2020 doi:10.20944/preprints202009.0532.v1

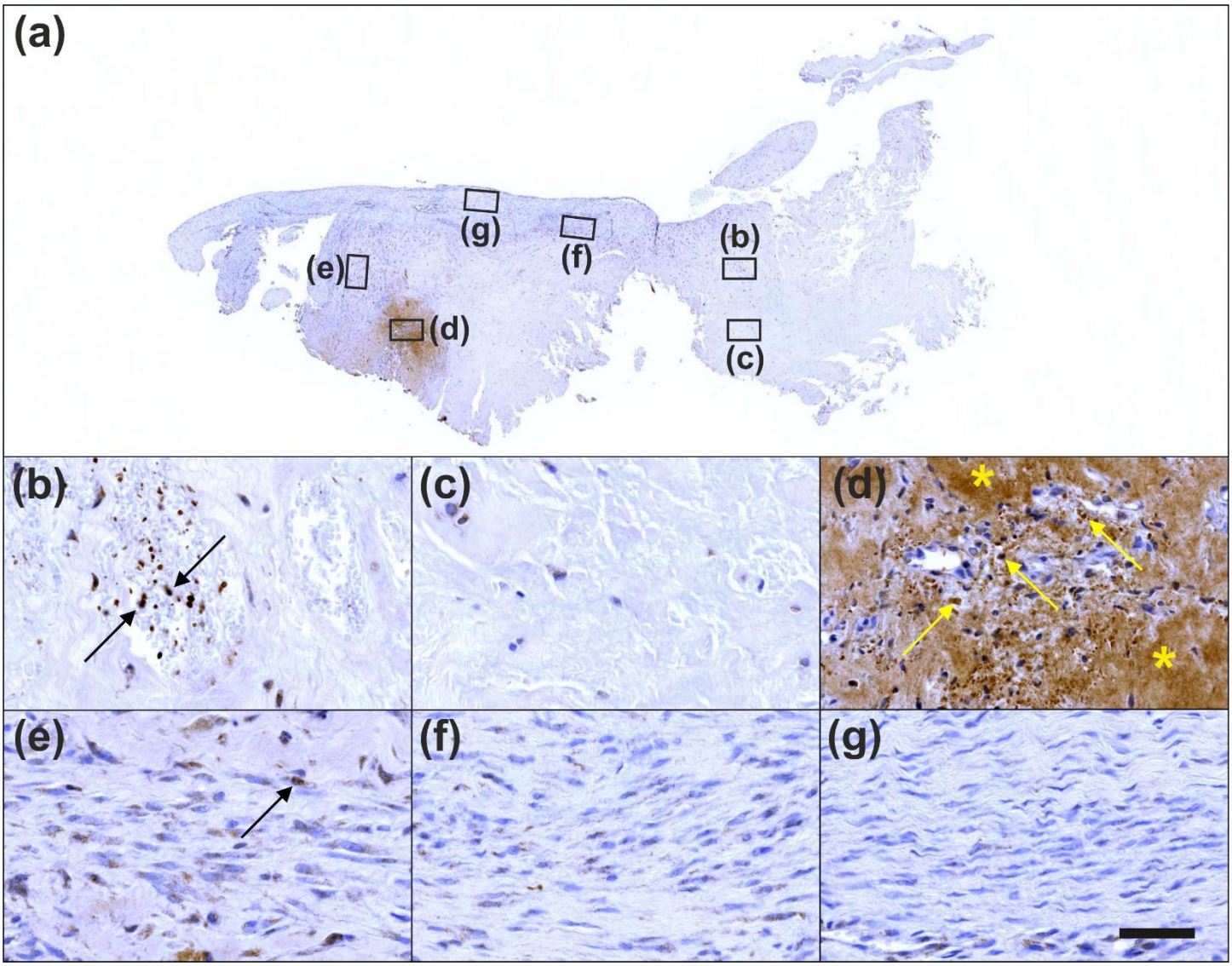

Figure 7. Immunohistochemical detection of tenomodulin in a section of the second part of the biopsy that was investigated in this study. The section was adjacent to the one shown in Figure 4(a); counterstaining was performed with Mayer's hematoxylin. The insets in (a) indicate the position of the high-power photomicrographs shown in (b-g), representing the same regions as the high-power photomicrographs shown in Figure 4(b-g). Intracellular immunolabeling for tenomodulin was found in Region d (yellow arrows in (d)), in some cells inside microvessels in Region b (black arrows in (b)) and in a very few cells in Region e (black arrow in (e)). Furthermore, extracellular immunolabeling for tenomodulin was abundantly observed in Region d (yellow asterisks in (d)). No immunolabeling for tenomodulin was found in Regions c, f and g. The scale bar in (g) represents 630 µm in (a) and 50 µm in (b-g).

A recent study suggested that in tendons, MMP-9 is specifically involved in debridement of individual collagen fibrils following tendon overload injury, and prior to deposition of new collagen (Baldwin et al., 2019). This is in line with an earlier study that demonstrated that MMP-9 is involved in tissue degradation during the early phase of healing, whereas MMP-2 contributes to tissue degradation and later remodeling (Oshiro et al., 2003). Another recent study on tenocyte-like cells isolated from biopsies of torn supraspinatus tendons from donors undergoing arthroscopic or open shoulder surgery found an approximately 20,000 times higher mean relative mRNA level of MMP-2 than of MMP-9 (Klatte-Schulz et al., 2015). However, neither individual nor average time intervals between occurence/diagnosis of tendon tear and surgery were reported in this study (Klatte-Schulz et al., 2015). Collectively, these data can explain why almost no MMP-9 immunolabeling was found in the second part of the investigated biopsy (Fig. 12).

CD68 is highly expressed by circulating macrophages and tissue macrophages (Vannella et al., 2017). By producing a variety of growth factors (including IGF-1, VEGF-α, TGF-β and Wnt proteins) that regulate, among others, differentiation of stem and tissue progenitor cells, proliferation of endothelial cells, activation of myofibroblasts and angiogenesis,

macrophages play an important role in regulating tissue regeneration following injury (Vannella and Wynn, 2017). Thus, the presence of CD68 immunopositive cells particularly in Region D (and, to a lesser extent, in Region E) of the second part of the investigated biopsy (Fig. 13d,e) support the hypothesis that Region D represented the site of injection of UA-ADRCs from where tendon regeneration began and was orchestrated.

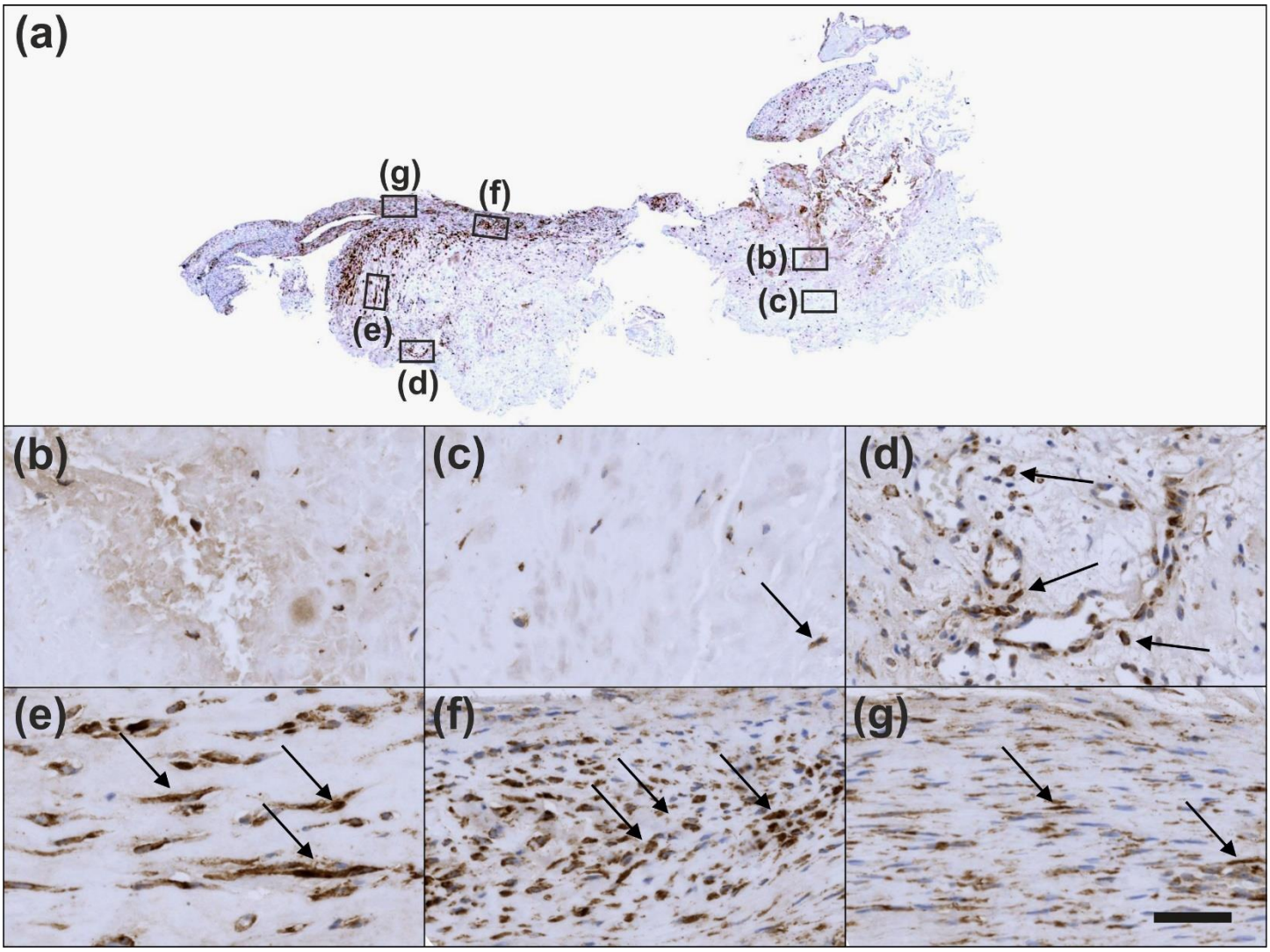

Figure 8. Immunohistochemical detection of type I procollagen in a section of the second part of the biopsy that was investigated in this study. The section was adjacent to the one shown in Figure 4(a); counterstaining was performed with Mayer's hematoxylin. The insets in (a) indicate the position of the high-power photomicrographs shown in (b-g), representing the same regions as the high-power photomicrographs shown in Figure 4(b-g). Immunolabeling for type I procollagen was found in a very few cells in Regions c and g, many cells outside microvessel walls in Region d, and in most cells in Regions e and f (black arrows in (c-g)). No immunolabeling for type I procollagen was found in Region b. The scale bar in (g) represents 630 µm in (a) and 50 µm in (b-g).

DISCUSSION

To our knowledge this is the first report demonstrating true regenerative healing of a partial-thickness tear in a human tendon following injection of UA-ADRCs. This is evidenced by comprehensive histological and immunohistochemical analysis of a biopsy taken from this tendon ten weeks post stem cell treatment.

With respect to the latter, the morphological appearance of Regions 3 and 4 in Figure 3 and Regions (b) and (c) in Figures 4-13 is in line with descriptions of the morphological appearance of degenerative supraspinatus tendon tissue at various degrees in the literature (Hashimoto et al., 2003; Lakemeier et al., 2010; Ferrer et al., 2019). Additionally, to our knowledge, spots within tendons with morphological appearance and immunohistochemical characterization as the one observed in the second part of the biopsy (Panels (d) in Figures 4-13) have not previously been described in the scientific literature. Besides this, in both parts of the biopsy the morphological appearance of those regions is characterized by elongated fibroblast-like cells arranged in

long and parallel chains between collagen fibers (Fig. 2b; Panels (e-g) in Figs 4-13). Organized, slightly undulating type I collagen (Region 1 in Figure 3) is consistent with descriptions of the morphological appearance of a process that is known as "regenerative healing in tendons without scar formation" in the literature (Beredjiklian et al., 2003; Tang et al., 2014; Galatz et al., 2015). Of note, this process does not occur in spontaneous tendon healing which typically results in a localized scar defect adjacent to intact enthesis (Beredjiklian et al., 2003; Tang et al., 2014; Moser et al., 2018). Rather, regenerative healing without scar formation so far has been attributed to fetal tendons (Beredjiklian et al., 2003; Tang et al., 2014; Galatz et al., 2015).

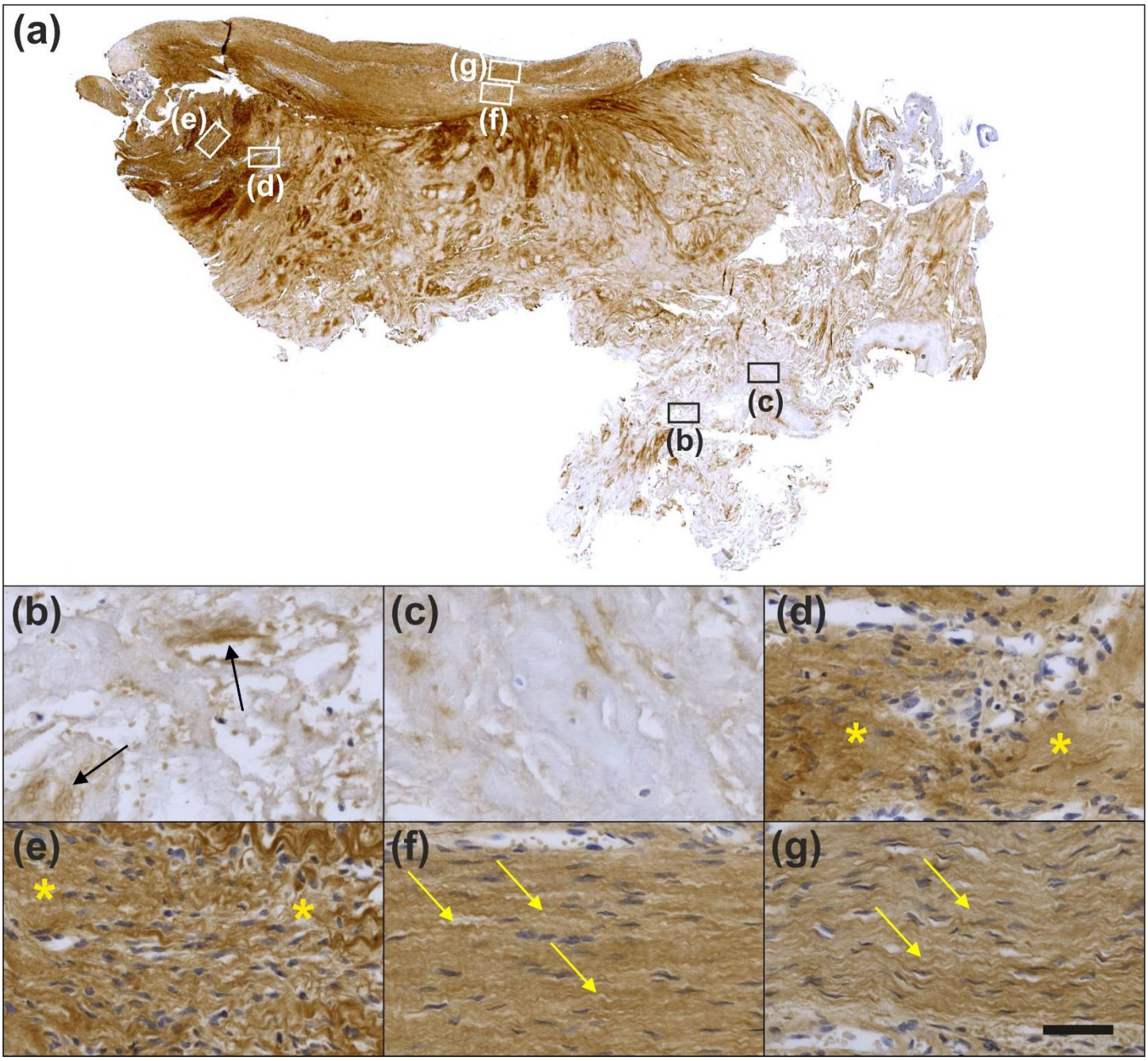

Figure 9. Immunohistochemical detection of type I collagen in a section of the second part of the biopsy that was investigated in this study. The section was adjacent to the one shown in Figure 4(a); counterstaining was performed with Mayer's hematoxylin. The insets in (a) indicate the position of the high-power photomicrographs shown in (b-g), representing the same regions as the high-power photomicrographs shown in Figure 4(b-g). Immunolabeling for unorganized type I collagen was found in Regions d and e (yellow asteriks in (d, e)), and to a small extent in Region b (black arrows in (b)). Organized, slightly undulating type I collagen was observed in Regions f and g (yellow arrows in (f, g)). The scale bar in (g) represents 630 µm in (a) and 50 µm in (b-g).

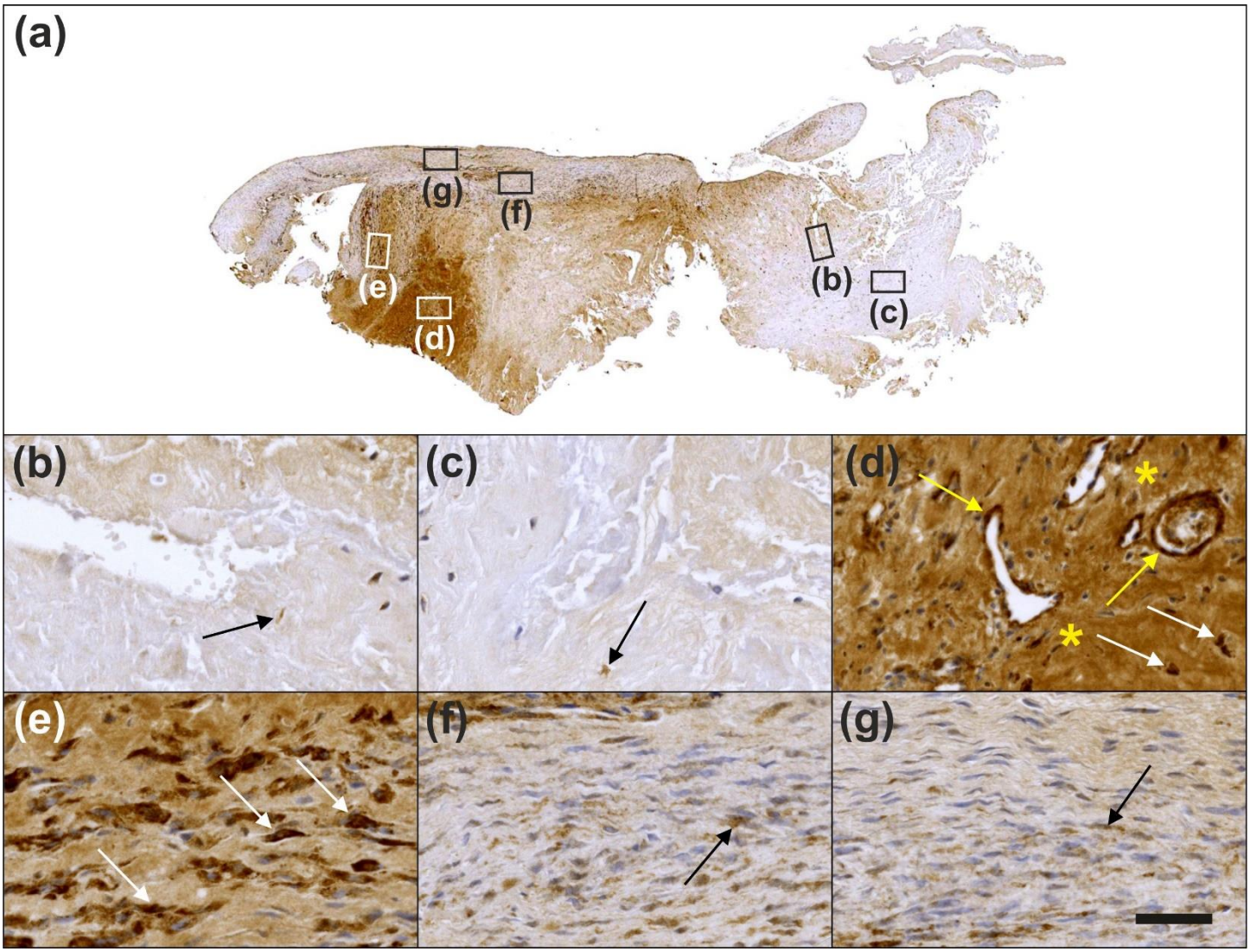

Figure 10. Immunohistochemical detection of laminin in a section of the second part of the biopsy that was investigated in this study. The section was adjacent to the one shown in Figure 4(a); counterstaining was performed with Mayer's hematoxylin. The insets in (a) indicate the position of the high-power photomicrographs shown in (b-g), representing the same regions as the high-power photomicrographs shown in Figure 4(b-g). Immunolabeling for laminin was found in a very few cells in Regions b, c, f and g (black arrows in (b, c, f, g)), and in many cells inside and outside microvessel walls in Regions d and e (yellow and white arrows in (d, e)). Furthermore, extracellular immunolabeling for laminin was abundantly observed in Region d (yellow asterisks in (d)). The scale bar in (g) represents 630 µm in (a) and 50 µm in (b-g).

In animal models, injections of adult stem cells isolated from adipose tissue into pathologic tendon tissue has produced a positive biological response (Kim et al., 2014; Valencia Mora et al., 2014; Chen et al., 2015; Gumucio et al., 2016; Tsekes et al., 2019). Reported beneficial effects include a decreased number of inflammatory cells, improved regeneration of tendons with less scarred healing, improved collagen fiber arrangement, higher load-to-failure and higher tensile strength of the treated tendons (Kim et al., 2014; Valencia Mora et al., 2014; Chen et al., 2015; Gumucio et al., 2016; Tsekes et al., 2019). These findings support the results we obtained by investigating a biopsy of a human tendon ten weeks post injection of UA-ADRCs. Our comprehensive immunohistochemical analysis of the biopsy with a broad number of antibodies (Tables 1 and 2) allow the conclusion that Region (d) in the second part of the biopsy (Panels (d) in Figs 4-13) represented the site of injection of UA-ADRCs from where tendon regeneration started. It further indicates that endothelial precursors and tenocytes might have migrated from Region (d) (where they were generated) via Region (f) to Region (f), in which tendon regeneration took place. Induction of differentiation and re-confirmation were most probably guided by complex signals released and communicated from the local microenvironment (Dong et al., 2015; Wabik and Jones, 2015; Alt et al., 2020).

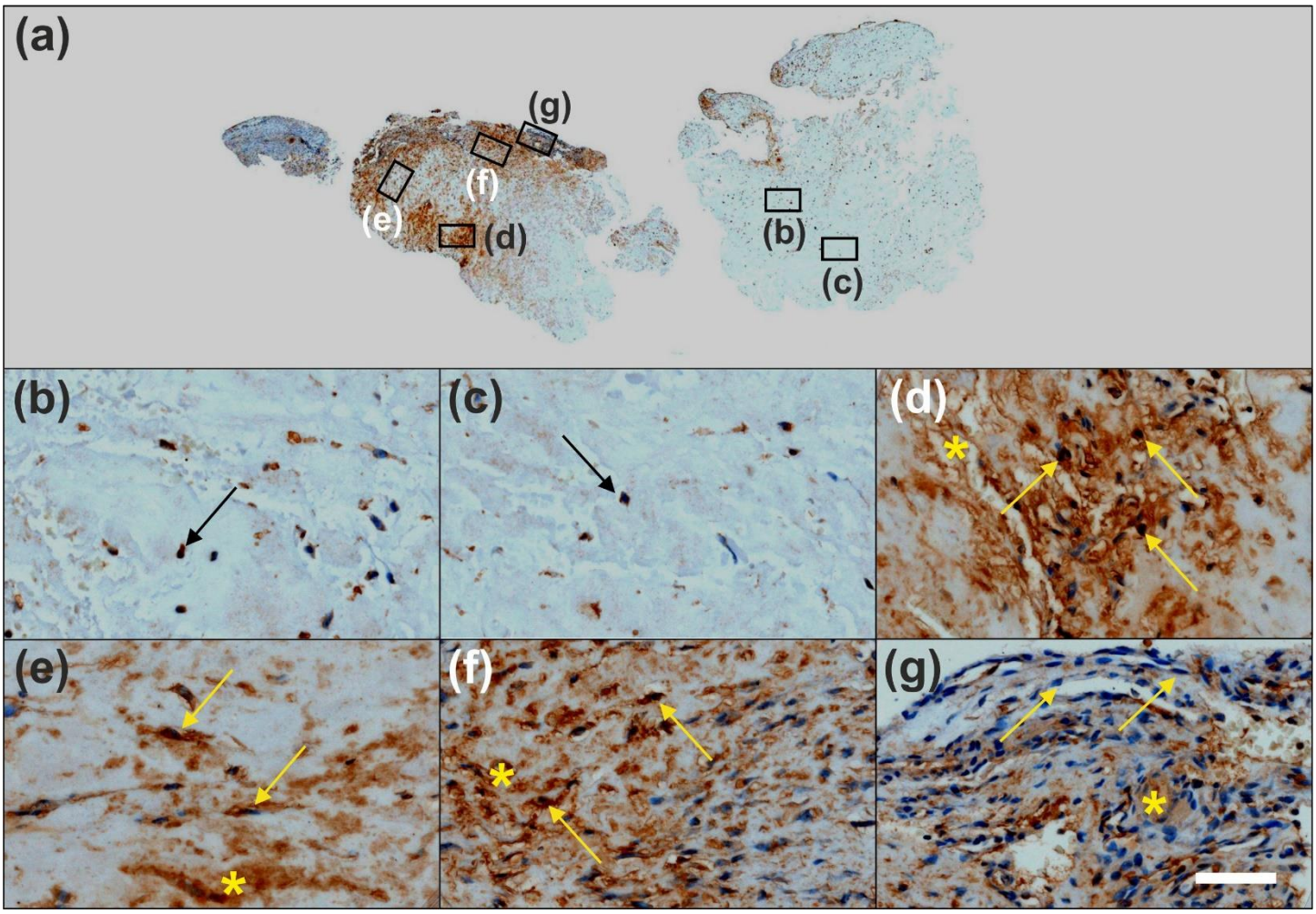

Figure 11. Immunohistochemical detection of matrix metalloproteinase 2 (MMP-2) in a section of the second part of the biopsy that was investigated in this study. The section was adjacent to the one shown in Figure 4(a); counterstaining was performed with Mayer's hematoxylin. The insets in (a) indicate the position of the high-power photomicrographs shown in (b-g), representing the same regions as the high-power photomicrographs shown in Figure 4(b-g). Intracellular MMP-9 immunolabeling was found in a few cells in Regions b-d, f and g (black arrows in (b-d, f, g) but not in Region e. No distinct extracellular MMP-9 immunolabeling was observed. The scale bar in (g) represents 630 µm in (a) and 50 µm in (b-g).

Some authors raised concerns about the use of ASCs/ADRCs in tendon regeneration due to their assumed "indigenous" preference towards forming adipocytes' (Docheva et al., 2015; Qi et al., 2020), albeit without reference to corresponding findings in the literature. We did not observe formation of adipocytes in the investigated biopsy. The latter result is in line with an earlier finding of our group clearly demonstrating that UA-ADRCs do *not* form adipocytes when used for treating chronic myocardial infarction (Haenel et al., 2019). Furthermore, in guided bone regeneration using UA-ADRCs we found substantially less formation of adipocytes (only 2% with stem cells) than without the use of UA-ADRCs (18%) (Solakoglu et al., 2019). Collectively, these findings do not only support the role of the local microenvironment for induction and guidance of differentiation of stem cells in the target tissue, but also underscore the need to exercise caution in drawing conclusions absent of convincing scientific evidence, or without a correct understanding of stem cell biology.

Conclusions of this study are presented on the basis of a single time point analysis of molecular and cellular events. As such, limitations consist in the fact that only a single subject was investigated; no control biopsy was analyzed, and the scientists who analyzed the biopsy were not blinded. It further was not the aim of the present study to establish a clinical treatment. To more conclusively evaluate clinical results with UA-ADRCs for incomplete tendon tears, a respective pivotal RCT is now recruiting (Hurd, 2018) based on encouraging clinical results of the pilot study (Hurd et al., 2020).

In summary, the results of this study indicate, for the first time, that treatment of an injured human tendon with unmodified, autologous regenerative cells can enable true regenerative healing. This process has previously been attributed only to fetal tendon development. It is of special importance that this success was achieved without prior manipulation, stimulation and/or (genetic) reprogramming of the cells injected.

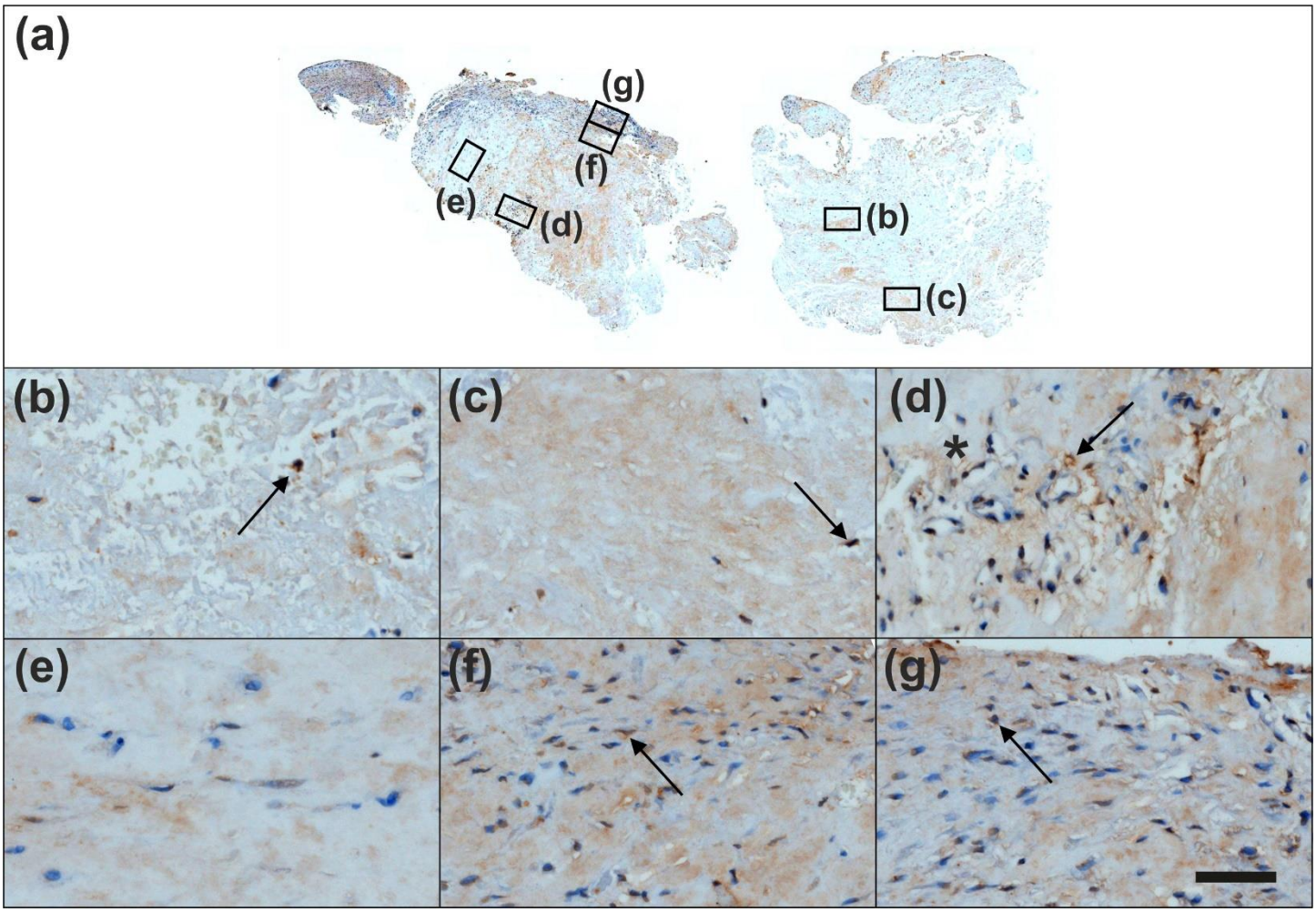

Figure 12. Immunohistochemical detection of matrix metalloproteinase 9 (MMP-9) in a section of the second part of the biopsy that was investigated in this study. The section was adjacent to the one shown in Figure 4(a); counterstaining was performed with Mayer's hematoxylin. The insets in (a) indicate the position of the high-power photomicrographs shown in (b-g), representing the same regions as the high-power photomicrographs shown in Figure 4(b-g). Intracellular MMP-2 immunolabeling was found in a few cells in Regions b, c and g (black arrows in (b, c) and yellow arrows in (g)), and in many cells in Regions d-f (yellow arrows in (d-f)). Extracellular MMP-2 immunolabeling was observed in Regions d-f and to a lesser extent in Region g (yellow arrows in (d-g)). The scale bar in (g) represents 630 µm in (a) and 50 µm in (b-g).

Acknowledgements
We thank Beate Aschauer, Andrea Haderer, Claudia Harbauer and Sabine Tost for excellent and highly valuable technical assistance; Dr. Maximilian Reiser for help in analyzing the MRI scans and Dr. Glenn Winnier for his support reviewing the manuscript.

Funding
This study was in part supported by the Alliance of Cardiovascular Researchers (New Orleans, LA, USA), by IsarKlinikum in Munich (Munich, Germany) and by InGeneron, Inc. (Houston, TX, USA). The sponsors of the study did not have any influence on data collection, analysis or publication. No constraints were placed on publication of the data.

Availability of data and materials
The data that support the findings of this study are available from the corresponding author upon reasonable request.

Authors' contributions
E.A. and C.S. designed the study. R.R. and M.H. performed the treatment. E.A., H.G.F., C.A. and C.S. collated the data and carried out data analysis. C.S. produced the initial draft of the manuscript. E.A., R.R., M.H., H.G.F. and C.A. contributed to drafting the manuscript. All authors have read and approved the final submitted manuscript.

Ethics approval and consent to participate
This study is a single self-experiment with the subject's consent. The subject was the first author of this study, Dr. Eckhard U. Alt, MD, PhD. Single self-experiments with the subject's unrestricted and free will formation are exempt from approval of an Institutional Review Board in Germany. It was Dr. Alt himself who initiated his own treatment, taking the biopsy and all investigations. Dr. Alt gave informed consent to participate in this study.

Consent for publication
We have obtained consent for publication.

Competing interests
Eckhard Alt is Executive Chair of InGeneron, Inc. (Houston, TX, USA) and Chairman of the Board of IsarKlinik AG. Ralf Rothoerl and Matthias

Hoppert are employed as medical doctors at IsarKlinikum. Christopher Alt is scientific director of InGeneron GmbH (Munich, Germany) which is owned by InGeneron, Inc. Christoph Schmitz serves as consultant to InGeneron, Inc.

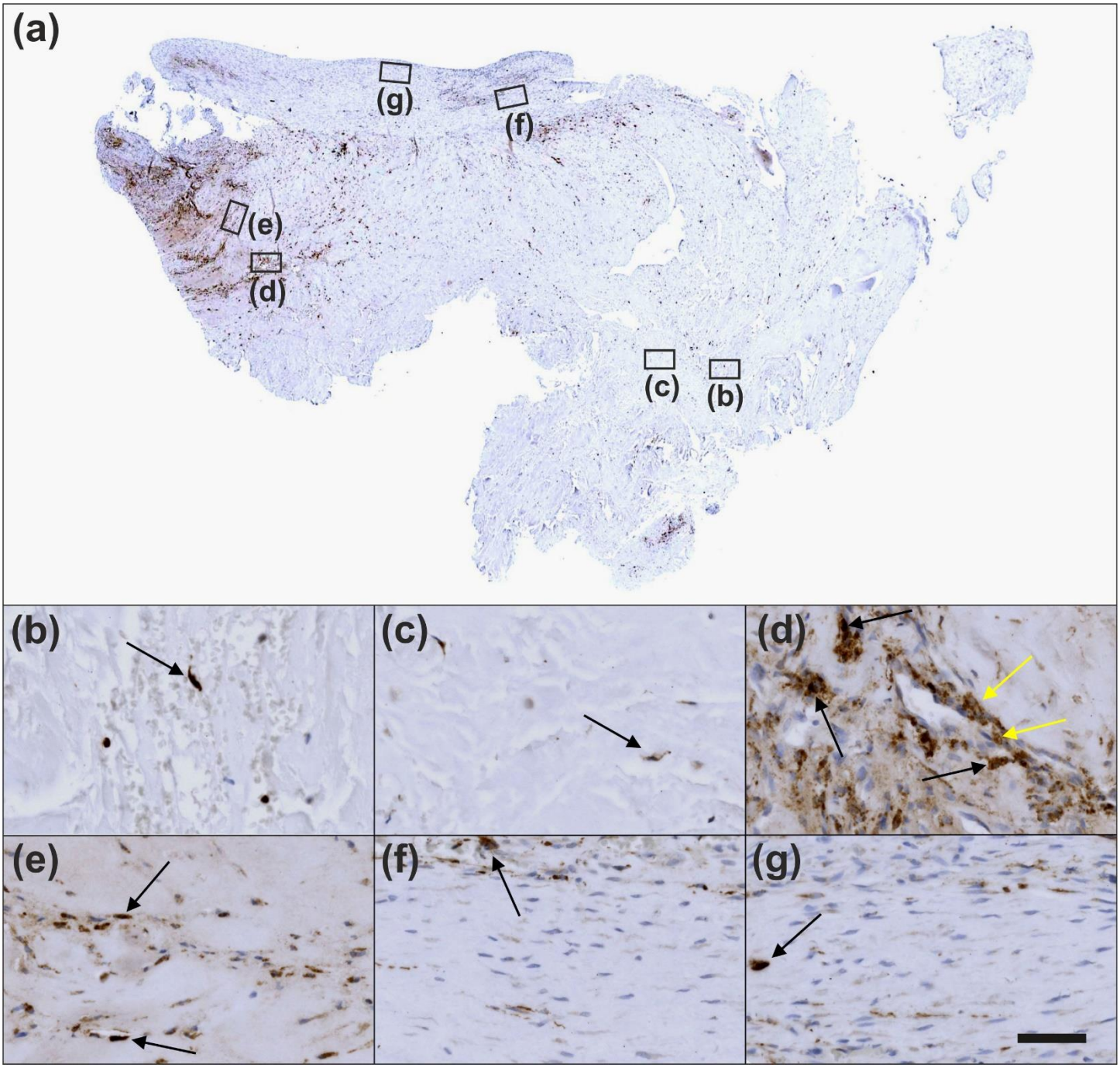

Figure 13. Immunohistochemical detection of CD68 in a section of the second part of the biopsy that was investigated in this study. The section was adjacent to the one shown in Figure 4(a); counterstaining was performed with Mayer's hematoxylin. The insets in (a) indicate the position of the high-power photomicrographs shown in (b-g), representing the same regions as the high-power photomicrographs shown in Figure 4(b-g). Immunolabeling for CD68 was found in a few cells in Regions b, c, e, f and g (black arrows in (b, c, e-g)) and more frequently in cells inside and outside microvessel walls in Region d (yellow and black arrows in (d)). The scale bar in (g) represents 630 µm in (a) and 50 µm in (b-g).

Table 2. Histological and immunohistochemical features of different regions within the second part of the biopsy that was investigated in this study.

Feature	Region in Figure 4						Fig.
	B	C	D	E	F	G	
Presence of microvessels	++	-	+++	(+)	-	-	4
Dense, unorganized cluster of cells and microvessels	-	-	+++	-	-	-	4
Elongated cells in a chain-like arrangement	-	-	-	++	+	+++	4
Immunohistochemical detection of…							
…CD34 in capillary endothelial cells	-	-	++	-	+++	+	5
…Ki-67 in cells inside microvessel walls	(+)	-	+++	-	-	-	6
…Ki-67 in cells outside microvessel walls	-	(+)	+++	-	+++	-	6
…intracellular tenomodulin	+	-	+++	(+)	-	-	7
… extracellular tenomodulin	-	-	+++	-	-	-	7
…type I procollagen	-	(+)	+++	+++	+++	+	8
…unorganized type I collagen	(+)	-	+++	+++	-	-	9
…organized, slightly undulating type I collagen	-	-	-	(+)	++	+++	9
…intracellular laminin	(+)	(+)	+++	+++	+	+	10
…extracellular laminin	-	-	+++	+	-	-	10
…intracellular MMP-2	(+)	(+)	+++	++	++	+	11
…extracellular MMP-2	-	-	+++	++	+++	+	11
…intracellular MMP-9	(+)	(+)	(+)	-	(+)	(+)	12
…extracellular MMP-9	-	-	-	-	-	-	12
…CD68	(+)	(+)	++	+	(+)	(+)	13

Absence or presence of individual features is coded as – (absence), (+) (minimal presence), + (slight presence), ++ (significant presence) and +++ (overwhelming presence). Column "Fig." indicates the corresponding figures in which detailed documentation is provided.

References

Aimes, R. T., & Quigley, J. P. (1995). Matrix metalloproteinase-2 is an interstitial collagenase. Inhibitor-free enzyme catalyzes the cleavage of collagen fibrils and soluble native type I collagen generating the specific 3/4- and 1/4-length fragments. *The Journal of Biological Chemistry*, 270(11), 5872–5876. doi: 10.1074/jbc.270.11.5872

Almalki, S. G., & Agrawal, D. K. (2016). Effects of matrix metalloproteinases on the fate of mesenchymal stem cells. *Stem Cell Research & Therapy*, 7(1), 129. doi: 10.1186/s13287-016-0393-1

Alt, E.U., Peters-Hall, J., Strobl, F., Easley, J., Seim, H. B., Kendall, L., Bens, C. Puttlitz, C., Gadomski, B., Alt, C., Winnier, G., & Schmitz, C. (2020). Tendon healing after treating tendon tears with autologous, unmodified stem cells: a combined magnetic resonance imaging / histology study using the rabbit Achilles tendon full transection model. *Submitted for publication*.

Alt, E.U., Schmitz, C., & Bai, X. Fundamentals of stem cells: why and how patients' own adult stem cells are the next generation of medicine. In: Bioethics and Research on Adult Stem Cells; Trafny, T., Spiri,S., Eds; IF Press: Pontifical Council for Culture, Rome, Italy, 2020; in press (preprint at doi: 10.20944/preprints201904.0200.v1).

Alt, E. U., Winnier, G., Haenel, A., Rothoerl, R., Solakoglu, O., Alt, C., & Schmitz, C. (2020). Towards a comprehensive understanding of UA-ADRCs (uncultured, autologous, fresh, unmodified, adipose derived regenerative cells, isolated at point of care) in regenerative medicine. *Cells*, 9(5), 1097. doi: 10.3390/cells9051097

Bajek, A., Gurtowska, N., Gackowska, L., Kubiszewska, I., Bodnar, M., Marszałek, A., Januszewski, R., Michalkiewicz, J., & Drewa, T. (2015). Does the liposuction method influence the phenotypic characteristic of human adipose-derived stem cells?. *Bioscience Reports*, 35(3), e00212. doi: 10.1042/BSR20150067

Baldwin, S. J., Kreplak, L., & Lee, J. M. (2019). MMP-9 selectively cleaves non-D-banded material on collagen fibrils with discrete plasticity damage in mechanically-overloaded tendon. *Journal of the Mechanical Behavior of Biomedical Materials*, 95, 67–75. doi: 10.1016/j.jmbbm.2019.03.020

Benjamin, M., & Ralphs, J. R. (1998). Fibrocartilage in tendons and ligaments--an adaptation to compressive load. *Journal of Anatomy*, 193 (Pt 4)(Pt 4), 481–494. doi: 10.1046/j.1469-7580.1998.19340481.x

Beredjiklian, P. K., Favata, M., Cartmell, J. S., Flanagan, C. L., Crombleholme, T. M., & Soslowsky, L. J. (2003). Regenerative versus reparative healing in tendon: a study of biomechanical and histological properties in fetal sheep. *Annals of Biomedical Engineering*, 31(10), 1143–1152. doi: 10.1114/1.1616931

Brandau, O., Meindl, A., Fässler, R., & Aszódi, A. (2001). A novel gene, tendin, is strongly expressed in tendons and ligaments and shows high homology with chondromodulin-I. *Developmental Dynamics*, 221(1), 72–80. doi: 10.1002/dvdy.1126

Chen, H. S., Su, Y. T., Chan, T. M., Su, Y. J., Syu, W. S., Harn, H. J., Lin, S. Z., & Chiu, S. C. (2015). Human adipose-derived stem cells accelerate the restoration of tensile strength of tendon and alleviate the progression of rotator cuff injury in a rat model. *Cell Transplantation*, 24(3), 509–520. doi: 10.3727/096368915X686968

Coombes, B. K., Bisset, L., & Vicenzino, B. (2010). Efficacy and safety of corticosteroid injections and other injections for management of tendinopathy: a systematic review of randomised controlled trials. *Lancet*, 376(9754), 1751–1767. doi: 10.1016/S0140-6736(10)61160-9

Cossu, G., Birchall, M., Brown, T., De Coppi, P., Culme-Seymour, E., Gibbon, S., Hitchcock, J., Mason, C., Montgomery, J., Morris, S., Muntoni, F., Napier, D., Owji, N., Prasad, A., Round, J., Saprai, P., Stilgoe, J., Thrasher, A., & Wilson, J. (2018). Lancet Commission: Stem cells and regenerative medicine. *Lancet*, 391(10123), 883–910. doi: 10.1016/S0140-6736(17)31366-1

Dex, S., Lin, D., Shukunami, C., & Docheva, D. (2016). Tenogenic modulating insider factor: Systematic assessment on the functions of tenomodulin gene. *Gene*, 587(1), 1–17. doi: 10.1016/j.gene.2016.04.051

Docheva, D., Müller, S. A., Majewski, M., & Evans, C. H. (2015). Biologics for tendon repair. *Advanced Drug Delivery Reviews*, 84, 222–239. doi: 10.1016/j.addr.2014.11.015

Dominici, M., Le Blanc, K., Mueller, I., Slaper-Cortenbach, I., Marini,

F., Krause, D., Deans, R., Keating, A., Prockop, D. j., & Horwitz, E. (2006). Minimal criteria for defining multipotent mesenchymal stromal cells. The International Society for Cellular Therapy position statement. *Cytotherapy*, 8(4), 315–317. doi: 10.1080/14653240600855905

Dong, L., Hao, H., Han, W., & Fu, X. (2015). The role of the microenvironment on the fate of adult stem cells. *Science China. Life Sciences*, 58(7), 639–648. doi: 10.1007/s11427-015-4865-9

Ferrer, G. A., Miller, R. M., Yoshida, M., Wang, J. H., Musahl, V., & Debski, R. E. (2020). Localized rotator cuff tendon degeneration for cadaveric shoulders with and without tears isolated to the supraspinatus tendon. *Clinical Anatomy*, 33(7), 1007–1013. doi: 10.1002/ca.23526

Galatz, L. M., Gerstenfeld, L., Heber-Katz, E., & Rodeo, S. A. (2015). Tendon regeneration and scar formation: The concept of scarless healing. *Journal of Orthopaedic Research*, 33(6), 823–831. doi: 10.1002/jor.22853

Gumucio, J. P., Flood, M. D., Roche, S. M., Sugg, K. B., Momoh, A. O., Kosnik, P. E., Bedi, A., & Mendias, C. L. (2016). Stromal vascular stem cell treatment decreases muscle fibrosis following chronic rotator cuff tear. *International Orthopaedics*, 40(4), 759–764. doi: 10.1007/s00264-015-2937-x

Haenel, A., Ghosn, M., Karimi, T., Vykoukal, J., Shah, D., Valderrabano, M., Schulz, D. G., Raizner, A., Schmitz, C., & Alt, E. U. (2019). Unmodified autologous stem cells at point of care for chronic myocardial infarction. *World Journal of Stem Cells*, 11(10), 831–858. doi: 10.4252/wjsc.v11.i10.831

Halper, J., & Kjaer, M. (2014). Basic components of connective tissues and extracellular matrix: elastin, fibrillin, fibulins, fibrinogen, fibronectin, laminin, tenascins and thrombospondins. *Advances in Experimental Medicine and Biology*, 802, 31–47. doi: 10.1007/978-94-007-7893-1_3

Hanley, B. P., Bains, W., & Church, G. (2019). Review of Scientific Self-Experimentation: Ethics History, Regulation, Scenarios, and Views Among Ethics Committees and Prominent Scientists. *Rejuvenation Research*, 22(1), 31–42. doi: 10.1089/rej.2018.2059

Hashimoto, T., Nobuhara, K., & Hamada, T. (2003). Pathologic evidence of degeneration as a primary cause of rotator cuff tear. *Clinical Orthopaedics and Related Research*, (415), 111–120. doi: 10.1097/01.blo.0000092974.12414.22

Hurd, J. (2018) Autologous adult adipose-derived regenerative cell injection into chronic partial-thickness rotator cuff tears. ClinicalTrials.gov Identifier: NCT03752827. Retrieved from https://www.clinicaltrials.gov/ct2/show/NCT03752827.

Hurd, J. L., Facile, T. R., Weiss, J., Hayes, M., Hayes, M., Furia, J. P., Maffulli, N., Winnier, G. E., Alt, C., Schmitz, C., Alt, E. U., & Lundeen, M. (2020). Safety and efficacy of treating symptomatic, partial-thickness rotator cuff tears with fresh, uncultured, unmodified, autologous adipose-derived regenerative cells (UA-ADRCs) isolated at the point of care: a prospective, randomized, controlled first-in-human pilot study. *Journal of Orthopaedic Surgery and Research*, 15(1), 122. doi: 10.1186/s13018-020-01631-8

Hurley, E. T., Hannon, C. P., Pauzenberger, L., Fat, D. L., Moran, C. J., & Mullett, H. (2019). Nonoperative treatment of rotator cuff disease with platelet-rich plasma: a systematic review of randomized controlled trials. *Arthroscopy*, 35(5), 1584–1591. doi: 10.1016/j.arthro.2018.10.115

Kim, S. H., Chung, S. W., & Oh, J. H. (2014). Expression of insulin-like growth factor type 1 receptor and myosin heavy chain in rabbit's rotator cuff muscle after injection of adipose-derived stem cell. *Knee Surgery, Sports Traumatology, Arthroscopy*, 22(11), 2867–2873. doi: 10.1007/s00167-013-2560-6

Klatte-Schulz, F., Aleyt, T., Pauly, S., Geißler, S., Gerhardt, C., Scheibel, M., & Wildemann, B. (2015). Do matrix metalloproteases and tissue inhibitors of metalloproteases in tenocytes of the rotator cuff differ with varying donor characteristics? *International Journal of Molecular Sciences*, 16(6), 13141–13157. doi: 10.3390/ijms160613141

Kukkonen, J., Joukainen, A., Lehtinen, J., Mattila, K. T., Tuominen, E. K., Kauko, T., & Aärimaa, V. (2014). Treatment of non-traumatic rotator cuff tears: A randomised controlled trial with one-year clinical results. *The Bone & Joint Journal*, 96-B(1), 75–81. doi: 10.1302/0301-620X.96B1.32168

Lakemeier, S., Reichelt, J. J., Patzer, T., Fuchs-Winkelmann, S., Paletta, J. R., & Schofer, M. D. (2010). The association between retraction of the torn rotator cuff and increasing expression of hypoxia inducible factor 1α and vascular endothelial growth factor expression: an immunohistological study. *BMC Musculoskeletal Disorders*, 11, 230. doi: 10.1186/1471-2474-11-230

Marvasti, T. B., Alibhai, F. J., Weisel, R. D., & Li, R. K. (2019). CD34+ stem cells: promising roles in cardiac repair and regeneration. *The Canadian Journal of Cardiology*, 35(10), 1311–1321. doi: 10.1016/j.cjca.2019.05.037

Matthewson, G., Beach, C. J., Nelson, A. A., Woodmass, J. M., Ono, Y., Boorman, R. S., Lo, I. K., & Thornton, G. M. (2015). Partial thickness rotator cuff tears: current concepts. *Advances in Orthopedics*, 2015, 458786. doi: 10.1155/2015/458786

Mescher, A.L. (2018) *Junqueira's basic histology text & atlas (*15th ed.). New York City, NY: McGraw-Hill Education.

Molloy, T. J., de Bock, C. E., Wang, Y., & Murrell, G. A. (2006). Gene expression changes in SNAP-stimulated and iNOS-transfected tenocytes--expression of extracellular matrix genes and its implications for tendon-healing. *Journal of Orthopaedic Research*, 24(9), 1869–1882. doi: 10.1002/jor.20237

Moser, H. L., Doe, A. P., Meier, K., Garnier, S., Laudier, D., Akiyama, H., Zumstein, M. A., Galatz, L. M., & Huang, A. H. (2018). Genetic lineage tracing of targeted cell populations during enthesis healing. *Journal of Orthopaedic Research*, 36(12), 3275–3284. doi: 10.1002/jor.24122

Oshiro, W., Lou, J., Xing, X., Tu, Y., & Manske, P. R. (2003). Flexor tendon healing in the rat: a histologic and gene expression study. *The Journal of Hand Surgery*, 28(5), 814–823. doi: 10.1016/s0363-5023(03)00366-6

Polly, S. S., Nichols, A., Donnini, E., Inman, D. J., Scott, T. J., Apple, S. M., Werre, S. R., & Dahlgren, L. A. (2019). Adipose-derived stromal vascular fraction and cultured stromal cells as trophic mediators for tendon healing. *Journal of Orthopaedic Research*, 37(6), 1429–1439. doi: 10.1002/jor.24307

Prockop, D. J., Kivirikko, K. I., Tuderman, L., & Guzman, N. A. (1979). The biosynthesis of collagen and its disorders (first of two parts). *The New England Journal of Medicine*, 301(1), 13–23. doi: 10.1056/NEJM197907053010104

Prockop, D. J., Kivirikko, K. I., Tuderman, L., & Guzman, N. A. (1979). The biosynthesis of collagen and its disorders (second of two parts). *The New England Journal of Medicine*, 301(2), 77–85. doi: 10.1056/NEJM197907123010204

Qi, F., Deng, Z., Ma, Y., Wang, S., Liu, C., Lyu, F., Wang, T., & Zheng, Q. (2020). From the perspective of embryonic tendon development: various cells applied to tendon tissue engineering. *Annals of Translational Medicine*, 8(4), 131. doi: 10.21037/atm.2019.12.78

Ramírez, J., Pomés, I., Cabrera, S., Pomés, J., Sanmartí, R., & Cañete, J. D. (2014). Incidence of full-thickness rotator cuff tear after subacromial corticosteroid injection: a 12-week prospective study. *Modern Rheumatology*, 24(4), 667–670. doi: 10.3109/14397595.2013.857798

Rezza, A., Sennett, R., & Rendl, M. (2014). Adult stem cell niches: cellular and molecular components. *Current Topics in Developmental Biology*, 107, 333–372. doi: 10.1016/B978-0-12-416022-4.00012-3

Scholzen, T., & Gerdes, J. (2000). The Ki-67 protein: from the known and the unknown. *Journal of Cellular Physiology*, 182(3), 311–322.

doi: 10.1002/(SICI)1097-4652(200003)182:3<311::AID-JCP1>3.0.CO;2-9

Schwitzguebel, A. J., Kolo, F. C., Tirefort, J., Kourhani, A., Nowak, A., Gremeaux, V., Saffarini, M., & Lädermann, A. (2019). Efficacy of platelet-rich plasma for the treatment of interstitial supraspinatus tears: a double-blinded, randomized controlled trial. *The American Journal of Sports Medicine*, 47(8), 1885–1892. doi: 10.1177/0363546519851097

Shukunami, C., Oshima, Y., & Hiraki, Y. (2001). Molecular cloning of tenomodulin, a novel chondromodulin-I related gene. *Biochemical and Biophysical Research Communications*, 280(5), 1323–1327. doi: 10.1006/bbrc.2001.4271

Solakoglu, Ö., Götz, W., Kiessling, M. C., Alt, C., Schmitz, C., & Alt, E. U. (2019). Improved guided bone regeneration by combined application of unmodified, fresh autologous adipose derived regenerative cells and plasma rich in growth factors: A first-in-human case report and literature review. *World Journal of Stem Cells*, 11(2), 124–146. doi: 10.4252/wjsc.v11.i2.124

Suh, H. N., & Han, H. J. (2010). Laminin regulates mouse embryonic stem cell migration: involvement of Epac1/Rap1 and Rac1/cdc42. *American Journal of Physiology. Cell Physiology*, 298(5), C1159–C1169. doi: 10.1152/ajpcell.00496.2009

Tang, Q. M., Chen, J. L., Shen, W. L., Yin, Z., Liu, H. H., Fang, Z., Heng, B. C., Ouyang, H. W., & Chen, X. (2014). Fetal and adult fibroblasts display intrinsic differences in tendon tissue engineering and regeneration. *Scientific Reports*, 4, 5515. doi: 10.1038/srep05515

Tsekes, D., Konstantopoulos, G., Khan, W. S., Rossouw, D., Elvey, M., & Singh, J. (2019). Use of stem cells and growth factors in rotator cuff tendon repair. *European Journal of Orthopaedic Surgery & Traumatology*, 29(4), 747–757. doi: 10.1007/s00590-019-02366-x

Valencia Mora, M., Antuña Antuña, S., García Arranz, M., Carrascal, M. T., & Barco, R. (2014). Application of adipose tissue-derived stem cells in a rat rotator cuff repair model. *Injury*, 45 Suppl 4, S22–S27. doi: 10.1016/S0020-1383(14)70006-3

Vannella, K. M., & Wynn, T. A. (2017). Mechanisms of organ injury and repair by macrophages. *Annual Review of Physiology*, 79, 593–617. doi: 10.1146/annurev-physiol-022516-034356

Wabik, A., & Jones, P. H. (2015). Switching roles: the functional plasticity of adult tissue stem cells. *The EMBO Journal*, 34(9), 1164–1179. doi: 10.15252/embj.201490386

Winnier, G. E., Valenzuela, N., Peters-Hall, J., Kellner, J., Alt, C., & Alt, E. U. (2019). Isolation of adipose tissue derived regenerative cells from human subcutaneous tissue with or without the use of an enzymatic reagent. *PloS One*, 14(9), e0221457. doi: 10.1371/journal.pone.0221457.